Supporting Info

for

A Selective Stepwise Heme Oxygenase Model System: Iron(IV)-Oxo Porphyrin π-Cation Radical Leads to a Verdoheme-Type Compound Via an Isoporphyrin Intermediate

Isaac Garcia-Bosch, Savita Sharma, Kenneth D. Karlin*.

Table of contents

hydroxide [2 mM]. **Black** spectrum: initial spectrum corresponding to (**1-SbF$_6$**) (λ_{max} = 523 nm); **purple** spectrum: recorded 10 seconds after addition of *m*CPBA, corresponding to formation of ($P^{Im\cdot+}$)Fe^{IV}=O (λ_{max} = 672 nm); **red/brown** spectra: decomposition of ($P^{Im\cdot+}$)Fe^{IV}=O) to a stable isoporphyrin complex (**2**) (λ_{max} = 825 and 920 nm) in the presence of water (**red**) or tetramethylammonium hydroxide (**brown**).

Figure S6. UV-Vis spectra following oxidation of (**5-SbF$_6$**) [0.2 mM] with *m*CPBA [1 mM] at -80 ºC in CH_2Cl_2 in the presence of water (3%) or tetrametthylammonium hydroxide [2 mM]. **Black** spectrum: initial spectrum corresponding to (**5-SbF$_6$**) (λ_{max} = 523 nm); **purple** spectrum: recorded 10 seconds after addition of *m*CPBA, corresponding to formation of ($F_8^{\cdot+}$)Fe^{IV}=O (λ_{max} = 656 nm); **red/brown** spectra: after decomposition of ($F_8^{\cdot+}$)Fe^{IV}=O giving a stable isoporphyrin complex (**2-F$_8$**) (λ_{max} = 825 and 920 nm) after warming the solution to 0 ºC in the presence of water (**red**) or tetramethylammonium hydroxide (**brown**).

Figure S7. UV-Vis spectra of oxidation of (**1-OH**) [0.1 mM] with CAN [40 mM] in a CH_3OH:H_2O (1:1) mixture. Black spectrum = initial spectra corresponding to (**1-OH**) (λ_{max} = 542 nm); red spectrum: 10 seconds after addition of CAN, corresponding to formation of isoporphyrin (λ_{max} = 929 nm); green spectra: transformation of isoporphyrin to final oxidation products (50% verdoheme (**4**) accumulation).

Figure S8. UV-Vis spectra of oxidation of (**1-OH**) [0.1 mM] with CAN [40 mM] in CH_3OH:CH_3CN (1:1) mixture. Black spectrum = initial spectra corresponding to (**1-OH**) (λ_{max} = 542 nm); red spectrum: 10 seconds after addition of CAN, corresponding to formation of isoporphyrin (λ_{max} = 910 nm); grey spectra: transformation of isoporphyrin to final oxidation products (no presence of verdoheme (**4**) UV-VIS features).

Figure S9. UV-Vis spectra of oxidation of (**1-OH**) [0.1 mM] with CAN [10 mM]. Top left: **Black** = initial spectrum corresponding to (**1-OH**) (560 nm); **red spectrum**: 10 seconds after addition of CAN, corresponding to formation of isoporphyrin (920 nm). Top right: **red spectrum**: isoporphyrin (**2**) and its transformation to intermediate species (**3**) (600-700 nm broad band, **grey spectra**). Bottom left: transformation of species (**3**) (**grey spectra**) to the final verdoheme-type complex (**4**) (**green spectrum**, (λ_{max} = 646 nm). Bottom right: kinetic traces demonstrating the clean sequential formation of (**1-OH**) to (**2**) (920 nm trace), (**3**) (615 nm trace) and (**4**) (646 nm trace).

Table S1. Reaction rates for the different reaction steps during oxidation of (**1-OH**) with CAN.

Figure S10. Top: time dependent traces of the absorbance at 615 nm (left) and 920 nm (right) during the oxidation of (**1-OH**) at different CAN concentrations [5 mM - 40 mM]. Bottom: time dependent traces of the absorbance at 615 nm (left) and 920 nm (right) during the oxidation of (**1-OH**) with CAN [20 mM] using H_2O or D_2O.

Table S2. Reaction rates for the different reaction steps during oxidation of (**5-OH**) with CAN.

Figure S26. ESI-MS spectra for the oxidation of (**1-OH**) with CAN [10 mM] in a (CH_3CN/H_2O) (direct injection of the reaction mixture). Top spectrum: average of the first reaction minute. Bottom spectrum: average spectrum from 5-10 minutes after addition of CAN.

Figure S27. ESI-MS spectra for the oxidation of (**1-OH**) with CAN [10 mM] in a ($CH_3CN/H_2{}^{18}\mathbf{O}$) (direct injection of the reaction mixture). Top spectrum: average of the first reaction minute. Bottom spectrum: average spectrum from 5-10 minutes after addition of CAN.

Figure S28. ESI-MS spectra for the oxidation of (**1-OH**) with CAN [10 mM] in a ($CH_3CN/H_2O/H_2{}^{18}\mathbf{O}$) (1:0.5:0.5) (direct injection of the reaction crude). Top spectrum: average of the first reaction minute. Bottom spectrum: average spectrum from 5-10 minutes after addition of CAN.

Figure S29. ESI-MS spectra for the oxidation of (**1-OH**) with CAN [10 mM] in a (CH_3CN/H_2O) in a saturated $^{18}\mathbf{O}_2$ atmosphere (direct injection of the reaction mixture). Top spectrum: average of the first reaction minute. Bottom spectrum: average spectrum from 5-10 minutes after addition of CAN.

Figure S30. ESI-MS spectra for the oxidation of (**1-OH**) with CAN [40 mM] in a (CH_3OH/H_2O) (direct injection of the reaction crude). Top spectrum: average of the first reaction minute. Bottom spectrum: average spectrum from 1 to 5 minutes after addition of CAN.

Figure S31. ESI-MS spectra for the oxidation of (**1-OH**) with CAN [40 mM] in a (CH_3CN /CH_3OH) (direct injection of the reaction crude). Top spectrum: average of the first reaction minute. Bottom spectrum: average spectrum from 1 to 5 minutes after addition of CAN.

Figure S32. ESI-MS spectra for the oxidation of (**5-OH**) with CAN [40 mM] in a (CH_3CN/H_2O) (direct injection of the reaction mixture). Top spectrum: average of the first reaction minute. Bottom spectrum: average spectrum from 5-10 minutes after addition of CAN.

Figure S33. ESI-MS spectra for the oxidation of (**5-OH**) with CAN [40 mM] in a ($CH_3CN/H_2{}^{18}O$) (direct injection of the reaction mixture). Top spectrum: average of the first reaction minute. Bottom spectrum: average spectrum from 5-10 minutes after addition of CAN.

1. Physical methods

All UV-VIS measurements were carried out by using a Hewlett Packard 8453 diode array spectrophotometer with a 10 mm path quartz cell. The spectrometer was equipped with a HP Chemstation software and Unisoku thermostated cell holder for low temperature experiments. Electrospray ionization mass spectroscopy (ESI-MS) spectra were acquired using a Finnigan LCQ Duo ion-trap mass spectrometer equipped with an electrospray ionization source (Thermo Finnigan, San Jose, CA). Electron paramagnetic resonance (EPR) spectra were recorded on a Bruker EMX spectrometer controlled with a Bruker ER 041 X G microwave bridge operating at X-band (~9.4 GHz). All NMR spectra were recorded in 7 inch, 5 mm o.d. NMR tubes. ^{2}H NMR was performed on Bruker 300 NMR instrument equipped with a tunable deuterium probe to enhance deuterium detection. The ^{2}H chemical shifts are calibrated to natural abundance deuterium solvent peaks.

2. Materials

All reagents and solvents purchased and used were of commercially available quality except as noted. Cerium ammonium nitrate 99.99% (CAN), sodium periodate 99.8% ($NaIO_4$) and labeled water 97% ^{18}O ($H_2{}^{18}O$) were obtained from Sigma-Aldrich. Acetonitrile, methanol and toluene were purified and dried by passing through an activated alumina purification system (Innovative Technology, Inc.). Deuterium oxide (D_2O) (D, 99.9%) was obtained from Cambridge Isotope Laboratories, Inc. $P^{Im}Fe^{III}(OH)$ (**1-OH**), $d_8P^{Im}Fe^{III}(OH)$ (**$d_8$1-OH**), $P^{Im}Fe^{III}(SbF_6)$ (**1-SbF$_6$**), $F_8Fe^{III}(OH)$ (**5-OH**), $F_8Fe^{III}(SbF_6)$ (**5-SbF$_6$**) and $d_8Fe^{III}(OH)$ (**$d_8$5-OH**) were synthesized as previously described.[1,2]

3. Isolation of products.

To a 60 mL acetonitrile:water mixture (1:1) containing 54 mg of $F_8Fe^{III}(OH)$ (**5-OH**) (1 mM) in an ice bath, 2.6 g of CAN [80mM] were added. After 3 minutes, the solution turned into a green color due to the formation verdoheme complex. At that point, the solution was added to an abstraction funnel that contained 30 mL of CH_2Cl_2. After filtration, the organic solution was dried under vacumm. 34 mg of a green powder was obtained, corresponding to the compound (**4-X**). Yield = 77%. UV-Vis [0.1 mM] in CH_3CN (λ, nm): 370, 390, 520, 622 (see **Figure S1**). ESI-MS (m/z): 703.1 (100), 720.1 (15). EPR in CH_3CN (g values): 6.03, 4.35, 1.99 (see **Figure S1**). Elemental analysis: ($C_{37}H_{17}F_6FeN_4O{\cdot}4H_2O{\cdot}CH_3CN{\cdot}CH_2Cl_2$) Calculated: C, 53.3%; H, 3.4%, N, 7.8%. Found: C, 53.6%; H, 3.4%; N, 7.2%.

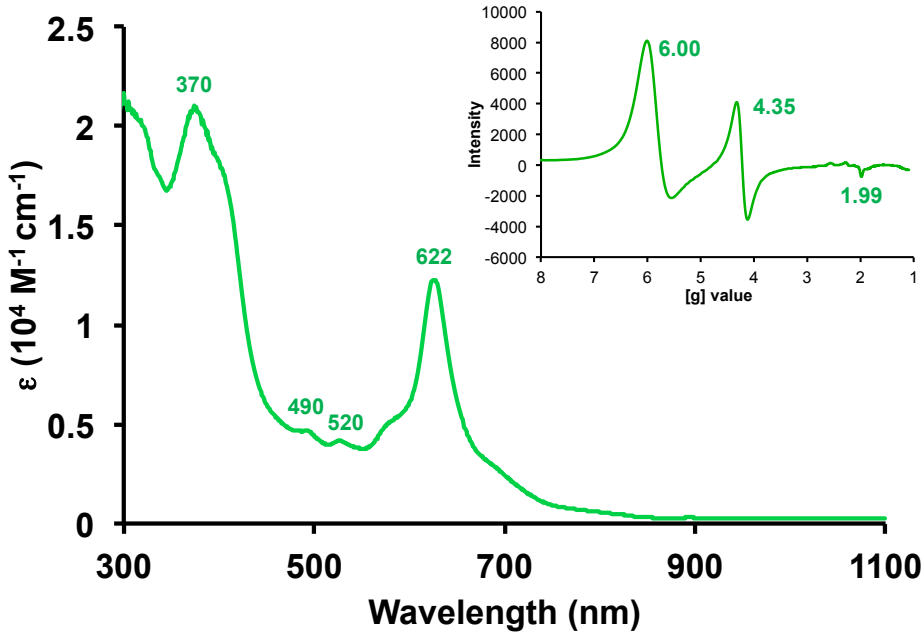

Figure S1. UV-Vis spectra of the isolated compound (**4-X**) [0.1 mM] in CH_3CN. Inset: EPR spectra of isolated compound (**4-X**) [3.0 mM] in CH_3CN.

4. UV-Vis experiments

In a typical experiment, 2.7 mL of a complex (**1-OH**) (0.1 mM) solution (CH_3CN/H_2O; 1:1) were placed in a 10 mm path quartz cell equipped with a stir bar. After cooling down to 0ºC, the desired quantity of CAN was dissolved in 1mL of H_2O and 0.3 mL of this aqueous solution were injected to the cell. To insure a homogenous addition, during the injection of CAN, Ar was bubbled through the solution. Spectra of the reaction were recorded every 5 seconds. For complex (**5-OH**), the same procedure was used. **Figure S2** showed the spectra recorded after addition of CAN [80 mM] into a solution containing (**5-OH**) [0.1 mM]. The proposed intermediates for the oxidation of (**5-OH**) are depicted in **Scheme S1**.

Oxidation of complexes (**1-OH**) and (**5-OH**) with sodium periodate ($NaIO_4$) led to the generation of stable Compound II-type species, with no further oxidation of the porphyrin (**Figures S3-S4**).[1,3]

A coupled oxidation of complexes (**1-OH**) and (**5-OH**) in a CH_3CN/H_2O (1:1) was also preformed, using ascorbic acid as an electron source and dioxygen. Although a color change was observed (purple-black change), no formation of verdoheme (**4-X**) product was observed (UV-Vis and ESI-MS analysis).

Oxidation of iron(III) complexes (**1-SbF_6**) and (**5-SbF_6**) using excess of *m*CPBA (5 equiv.) in CH_2Cl_2 at low temperature led to the formation of Compound I-type species which decomposed, due to the presence of water (3%), to stable isoporphyrin-type species (**Figures S5-S6**).[4-6] Generation of iron(IV)-oxo π-radical species in the presence of tetramethylammonium hydroxide [2 mM] also led to the generation of the same isoporphyrin-type species. Compound I-type species generated under these

conditions were also characterized by EPR spectroscopy, exhibiting distinctive and characteristic signals.[7] (NOTE: although Cmpd I-type species can be generated with little excess of *m*CPBA (1.5 equiv), 5 equiv. are required in these experiments for their full formation).

For complex (**1-SbF$_6$**), when we warmed up the solution we observed that the isoporphyrin formed was not stable and formation of (**1-OH**) as well as some bleaching process occurs (the same reversibility was observed by Fujii and coworkers, see ref. 17). After removing the CH_2Cl_2, the product was solved in CH_3CN:H_2O (1:1), and when CAN was added (40mM) forming the reaction product (**4-X**). For complex (**5-SbF$_6$**), the isoporphyrin compound was relatively stable in CH_2Cl_2 which allowed recording the UV-Vis spectrum (no same obtained at low temperature) and its ESI-MS analysis (only masses corresponding to the iron(III) complex were observed). However, when the isoporphyrin was dissolved in CH_3CN/H_2O, we observed the formation of the iron(III) complex (**5-OH**) as well as a bleaching process (decay of the intensity of Soret and Q-bands). After removing the CH_2Cl_2, the product was solved in CH_3CN:H_2O (1:1), and when CAN was added (40mM) forming the reaction product (**4-X**).

In order to corroborate that the isoporphyrin (**2**) is formed by nucleophilic attack of H_2O, we performed the oxidation of (**1-OH**) using different solvent mixtures: MeOH:H_2O (1:1) (**Figure S7**), MeOH:CH_3CN (1:1) (**Figure S8**). In the case of the MeOH:CH_3CN (1:1), we observe a shift in the isoporphyrin formed (λ_{max} = 910 nm), suggesting a different isoporphyrin is formed ((**1+(O(OMe))**, λ_{max} = 920 nm), that didn't lead to the formation of the verdoheme complex (**4**). When a MeOH:H_2O mixture was used, new isoporphyrin complexes (λ_{max} = 930 nm) were formed that led to the formation of verdoheme (**4**) complex (λ_{max} = 649 nm) with 50% of accumulation.

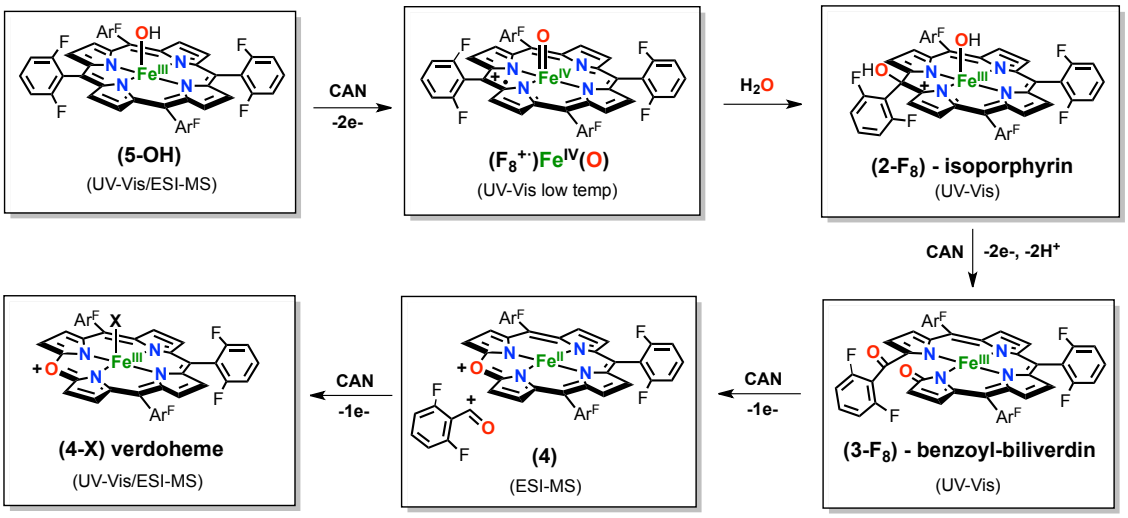

Scheme S1. Proposed mechanism for the oxidation of (**5-OH**) to verdoheme-type complex (**4-X**) via formation of isoporphyrin (**2-F$_8$**) and benzoyl-biliverdin (**3-F$_8$**).

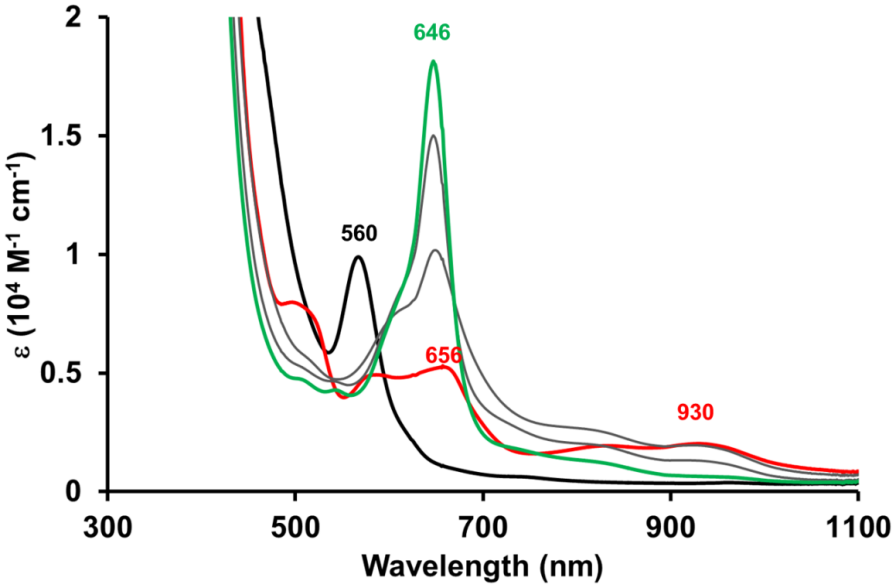

Figure S2. UV-Vis spectra of oxidation of (**5-OH**) [0.1 mM] with CAN [80 mM]. **Black** = initial spectrum corresponding to (**5-OH**) (λ_{max} = 560 nm); **red** spectrum: 10 seconds after addition of CAN, corresponding to formation of isoporphyrin (λ_{max} = 930 nm); **grey** spectrum: transformation of isoporphyrin to intermediate species (600-700 nm broad band) and final verdoheme-type complex (**4**) (**green** spectrum, (λ_{max} = 646 nm).

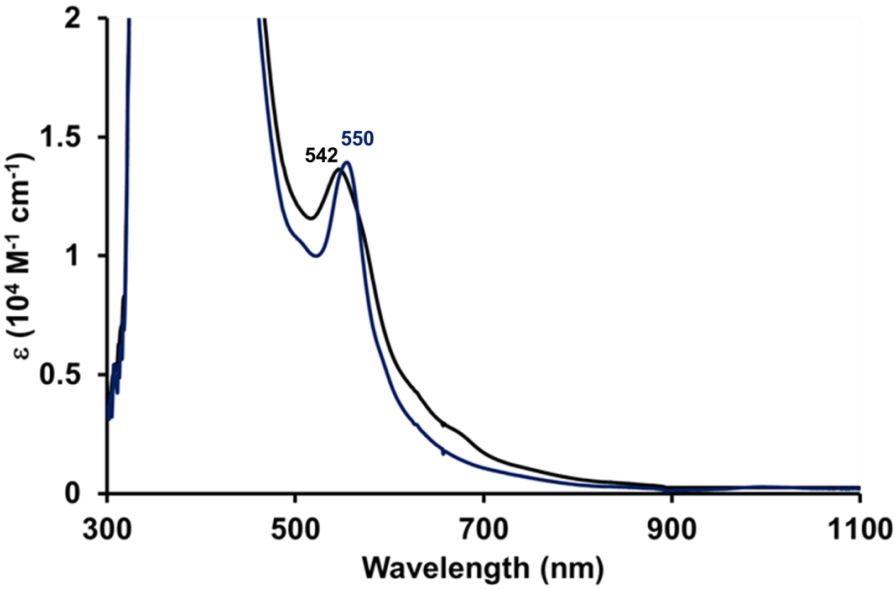

Figure S3. UV-Vis spectra for the oxidation of (**1-OH**) [0.1 mM] with $NaIO_4$ [40 mM]. **Black** spectrum = initial spectra corresponding to (**1-OH**) (λ_{max} = 542 nm); **blue** spectrum: (P)Fe^{IV}=O complex (Compound II-type) (λ_{max} = 550 nm).[1,3]

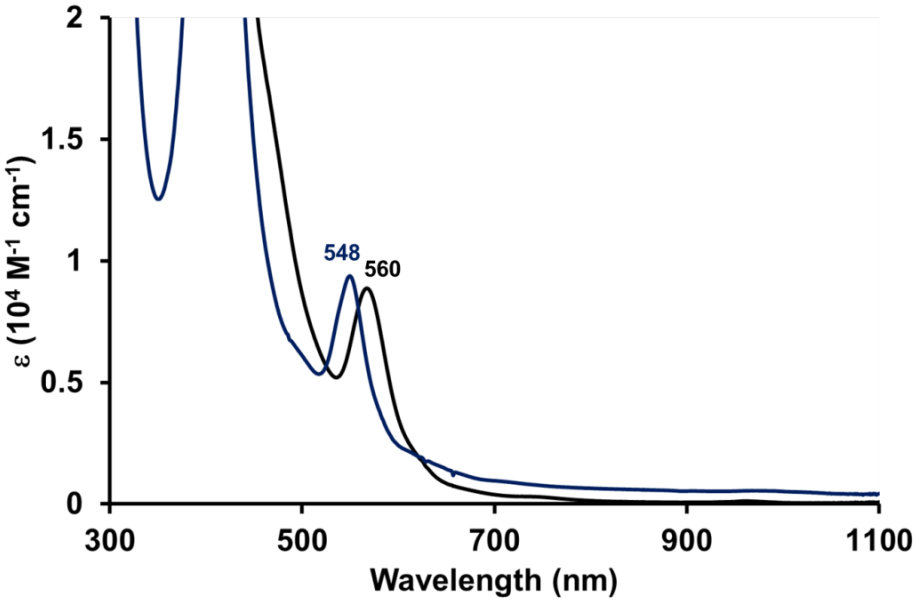

Figure S4. UV-Vis spectra of oxidation of (**5-OH**) [0.1 mM] with $NaIO_4$ [40 mM]. **Black** spectrum = initial spectrum corresponding to (**5-OH**) (λ_{max} = 560 nm); **blue** spectrum: $(P)Fe^{IV}=O$ complex (Compound II) (λ_{max} = 548 nm).

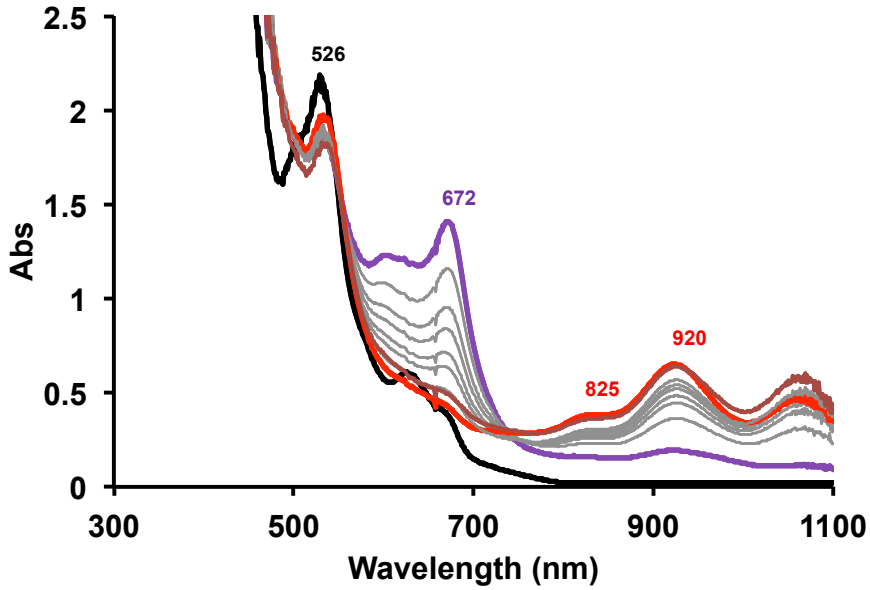

Figure S5. UV-Vis spectra following the oxidation of (**1-SbF$_6$**) [0.2 mM] with *m*CPBA [1 mM] at -80ºC in CH_2Cl_2 in the presence of water (3%) or tetramethylammonium hydroxide [2 mM]. **Black** spectrum: initial spectrum corresponding to (**1-SbF$_6$**) (λ_{max} = 523 nm); **purple** spectrum: recorded 10 seconds after addition of *m*CPBA, corresponding to formation of $(P^{Im\cdot+})Fe^{IV}=O$ (λ_{max} = 672 nm); **red/brown** spectra: decomposition of $(P^{Im\cdot+})Fe^{IV}=O$) to a stable isoporphyrin complex (**2**) (λ_{max} = 825 and 920 nm) in the presence of water (**red**) or tetramethylammonium hydroxide (**brown**).

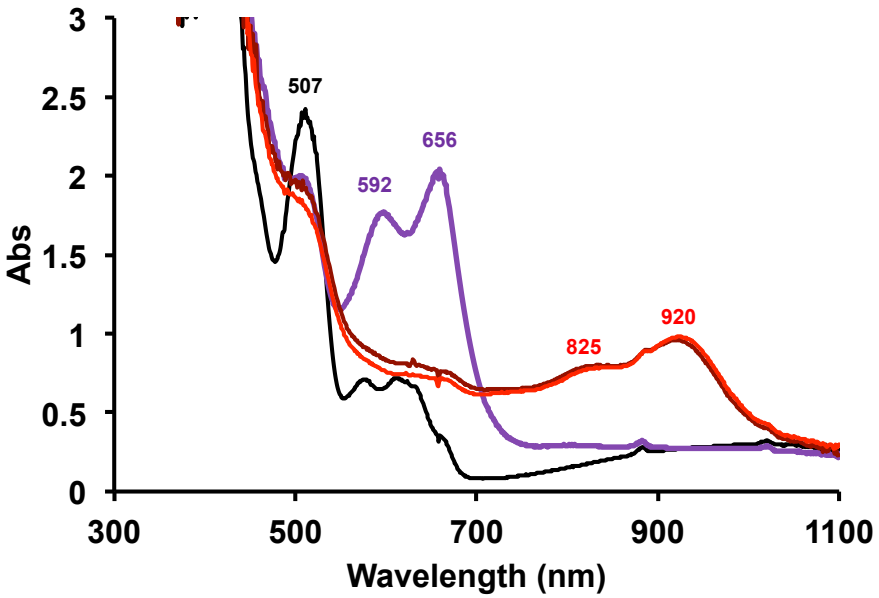

Figure S6. UV-Vis spectra following oxidation of (**5-SbF$_6$**) [0.2 mM] with *m*CPBA [1 mM] at -80 ºC in CH_2Cl_2 in the presence of water (3%) or tetrametthylammonium hydroxide [2 mM]. **Black** spectrum: initial spectrum corresponding to (**5-SbF$_6$**) (λ_{max} = 523 nm); **purple** spectrum: recorded 10 seconds after addition of *m*CPBA, corresponding to formation of ($F_8^{\cdot+}$)Fe^{IV}=O (λ_{max} = 656 nm); **red/brown** spectra: after decomposition of ($F_8^{\cdot+}$)Fe^{IV}=O giving a stable isoporphyrin complex (**2-F$_8$**) (λ_{max} = 825 and 920 nm) after warming the solution to 0 ºC in the presence of water (**red**) or tetramethylammonium hydroxide (**brown**).

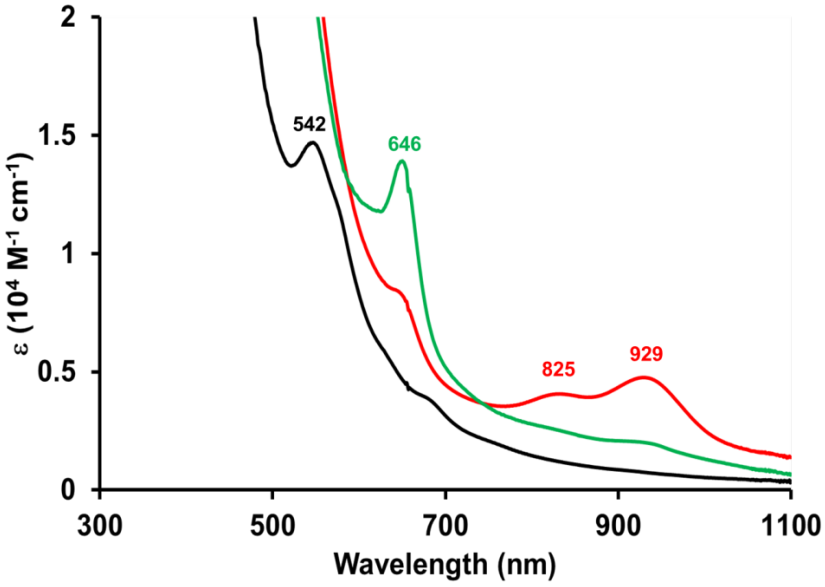

Figure S7. UV-Vis spectra of oxidation of (**1-OH**) [0.1 mM] with CAN [40 mM] in a CH_3OH:H_2O (1:1) mixture. Black spectrum = initial spectra corresponding to (**1-OH**) (λ_{max} = 542 nm)**; red** spectrum: 10 seconds after addition of CAN, corresponding to formation of isoporphyrin (λ_{max} = 929 nm); **green** spectra: transformation of isoporphyrin to final oxidation products (50% verdoheme (**4**) accumulation).

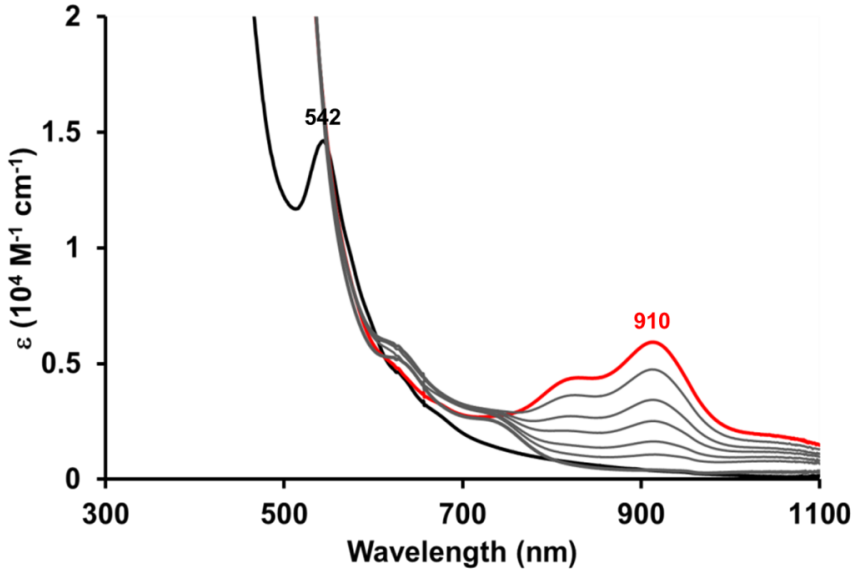

Figure S8. UV-Vis spectra of oxidation of (**1-OH**) [0.1 mM] with CAN [40 mM] in CH_3OH:CH_3CN (1:1) mixture. Black spectrum = initial spectra corresponding to (**1-OH**) (λ_{max} = 542 nm); **red** spectrum: 10 seconds after addition of CAN, corresponding to formation of isoporphyrin (λ_{max} = 910 nm); **grey** spectra: transformation of isoporphyrin to final oxidation products (no presence of verdoheme (**4**) UV-VIS features).

5. Kinetic experiments:

As for the regular UV-Vis experiments, 2.7 mL of a complex (**1-OH**) [0.1 mM] solution (CH_3CN/H_2O; 1:1) were placed in a 10 mm path quartz cell equipped with a stir bar. After cooling to 0 ºC, the desired quantity of CAN [1 mM – 40 mM] was dissolved in 1 mL of H_2O and 0.3 mL of this aqueous solution were injected to the cell with solution. To insure a homogenous addition, during the injection of CAN, argon was bubbled through the solution. UV-vis spectra of the reaction were recorded every 5 seconds. For complex (**5-OH**), the same procedure was used, using higher concentrations of CAN [1 mM - 100 mM]. Due to multiple steps involved in the formation of the different reaction intermediates (see **Figure S9**), the 'initial rate' approximation was used to determine the different reaction rates (**Tables S1-S2**). Time dependent traces for both complexes are shown in **Figures S10 –S11**. Comparisons of the different reaction rates calculated for both complexes are shown in **Figure S12**, with higher reaction rates for complex (**1-OH**) in all reaction steps at lower concentrations of CAN being observed.

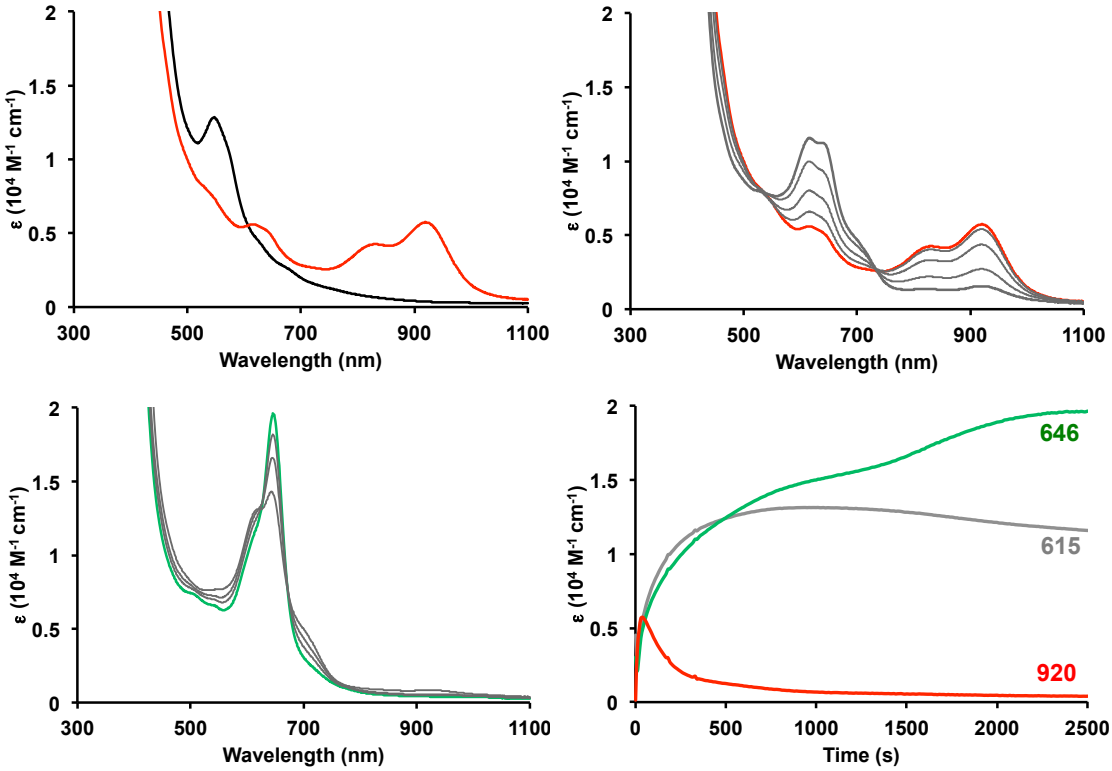

Figure S9. UV-Vis spectra of oxidation of (**1-OH**) [0.1 mM] with CAN [10 mM]. Top left: **Black** = initial spectrum corresponding to (**1-OH**) (560 nm); **red spectrum**: 10 seconds after addition of CAN, corresponding to formation of isoporphyrin (920 nm). Top right: **red spectrum**: isoporphyrin (**2**) and its transformation to intermediate species (**3**) (600-700 nm broad band, **grey spectra**). Bottom left: transformation of species (**3**) (**grey spectra**) to the final verdoheme-type complex (**4**) (**green spectrum**, (λ_{max} = 646 nm). Bottom right: kinetic traces demonstrating the clean sequential formation of (**1-OH**) to (**2**) (920 nm trace), (**3**) (615 nm trace) and (**4**) (646 nm trace).

Table S1. Reaction rates for the different reaction steps during oxidation of (**1-OH**) with CAN.

[CAN]	Rate formation (**2**) (10^{-7} M/s)	Rate decomp. (**2**) (10^{-7} M/s)	Rate formation (**4**) (10^{-7} M/s)
[5 mM]	26	-2.6	2.5
[10 mM]	31	-3.4	3.4
[20 mM]	48	-4.4	4.3
[20 mM] (D_2O)	34	-2.5	4.1
[40 mM]	50	-4.6	4.4

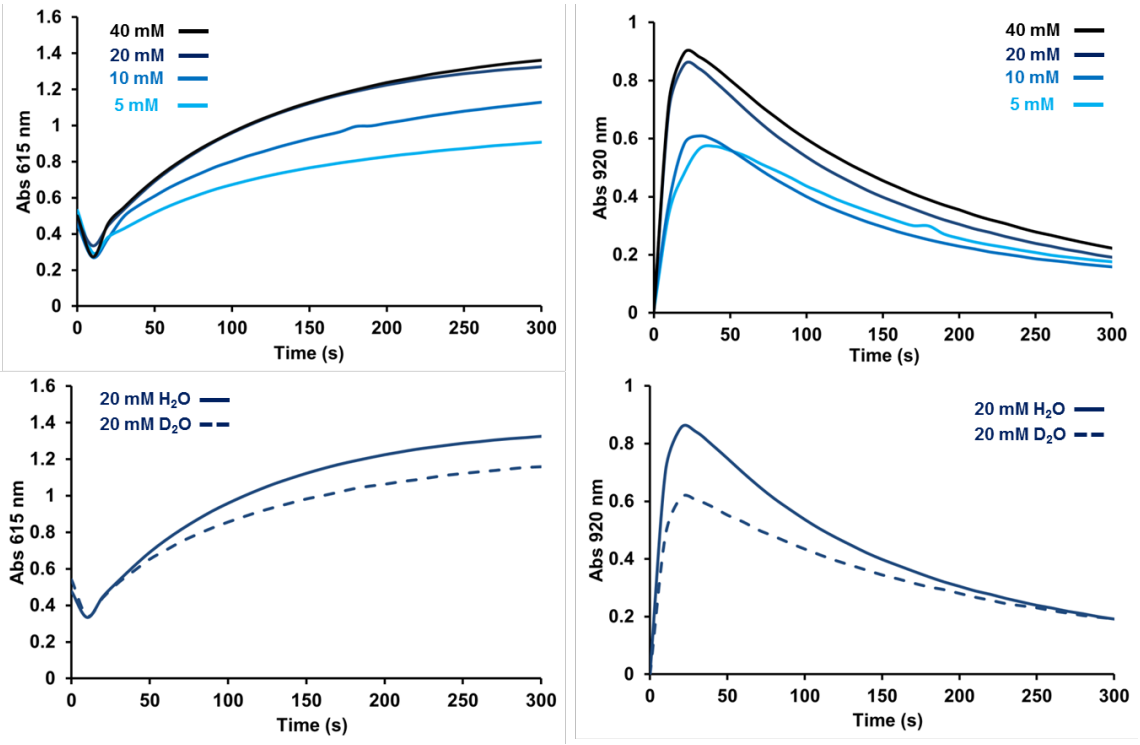

Figure S10. Top: time dependent traces of the absorbance at 615 nm (left) and 920 nm (right) during the oxidation of (**1-OH**) at different CAN concentrations [5 mM - 40 mM]. Bottom: time dependent traces of the absorbance at 615 nm (left) and 920 nm (right) during the oxidation of (**1-OH**) with CAN [20 mM] using H_2O or D_2O.

Table S2. Reaction rates for the different reaction steps during oxidation of (**5-OH**) with CAN.

[CAN]	Rate formation (2-F_8) (10^{-7} M/s)	Rate decomp. (2-F_8) (10^{-7} M/s)	Rate formation (**4**) (10^{-7} M/s)
[5 mM]	0	0	0
[10 mM]	0	0	0.02
[20 mM]	6	-0.5	0.08
[40 mM]	14	-0.8	0.5
[60 mM]	14	-0.9	1.5
[80 mM]	15	-1.8	2.2
[100 mM]	15	-2.1	2.6

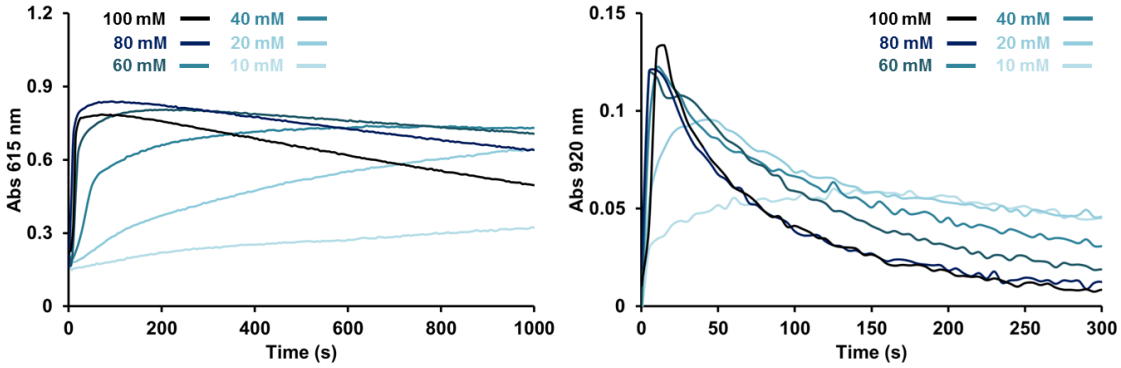

Figure S11. Time dependent traces of the absorbance at 615 nm (left) and 920 nm (right) during the oxidation of (**5-OH**) at different CAN concentrations [10 mM-100 mM].

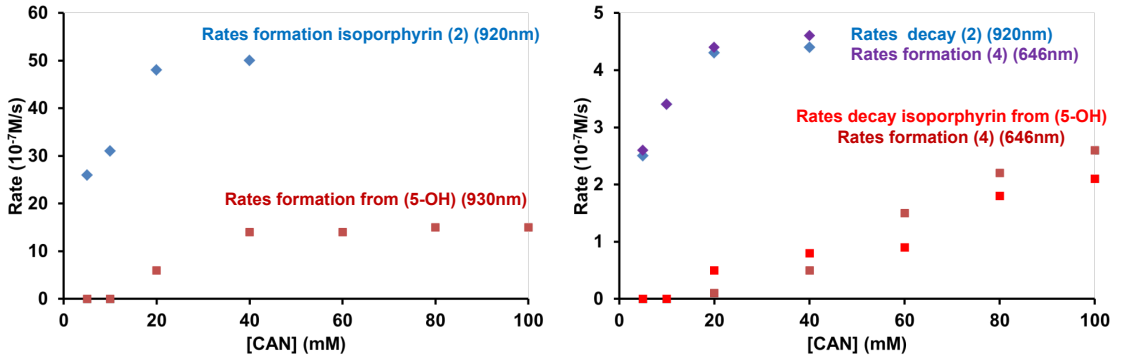

Figure S12. Comparison between reaction rates shown by complexes (**1-OH**) and (**5-OH**) and their oxidation with different concentrations of CAN. Left: reaction rates for the formation of isoporphyrin complexes. Right: reaction rates for the decay of isoporphyrin complexes (**2**) and (**2-F$_8$**) and formation of the final verdoheme complex (**4**).

6. EPR experiments.

Two different sets of EPR experiments were carried out.

0.57 mL of a complex (**1-SbF$_6$**) (3.0 mM) solution in CH_2Cl_2 were placed in two EPR tubes insight the glovebox and capped properly with rubber septa. One of the tubes was frozen in liquid N_2 and the EPR spectrum was recorded (**Figure S13**). The second tube was cooled down to -80 ºC in an acetone/dry ice bath and 0.03 mL of a *m*CPBA solution were added. The EPR tube was frozen and the spectrum was recorded at 14K (**Figure S14**). The same procedure was followed for the (**5-SbF$_6$**) (**Figures S15-S16**). Complex (**1-SbF$_6$**) showed two set of signals, a 6.02 [g] value which corresponds to an high-spin iron (III) compound and [g] = 2.92, 2.60, 2.30 values which can be assigned to a low-spin iron(III) compound. After addition of *m*CPBA, three new signals were observed, [g] = 4.29, 2.93, 2.00, which are assigned to the formation of a Cmpd-I type complex, interpreted as a weak ferromagnetic interaction between ferryl iron (S = 1) and the porphyrin π-cation radical (S = 1/2), although further studies are required to confirm the exact electronic structure of this compound.[7] For complex (**5-SbF$_6$**), [g]

values = 5.64 and 2.0 were found, typical of high-spin iron(III) complex. After addition of *m*CPBA, new [g] values were found (4.25, 3.75, 1.98), an EPR spectra typical of those of S = 3/2 systems, indicating strong ferromagnetic interactions between ferryl iron (S = 1) and the porphyrin π-cation radical (S = 1/2).

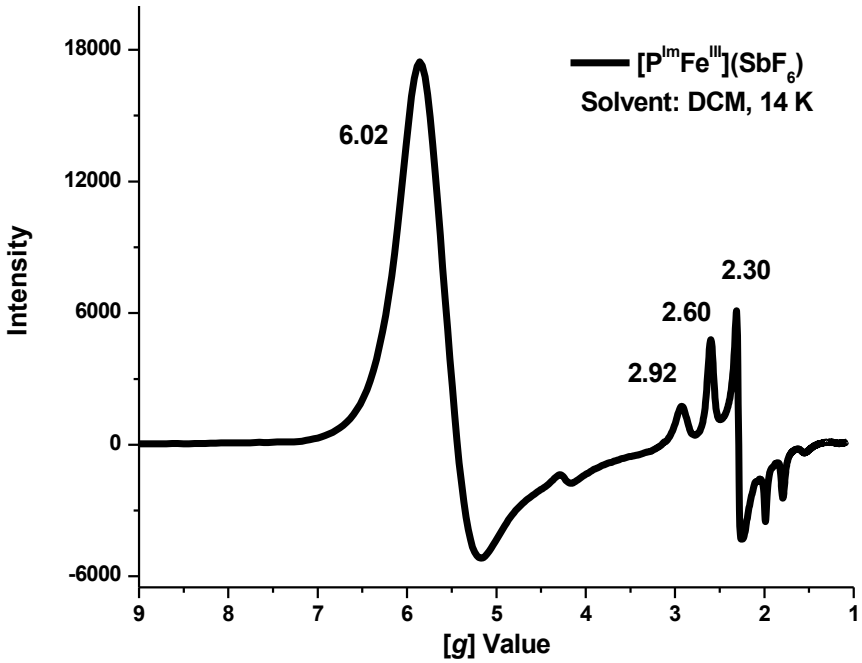

Figure S13. EPR of complex (**1-SbF$_6$**) [3.0 mM] in CH_2Cl_2.

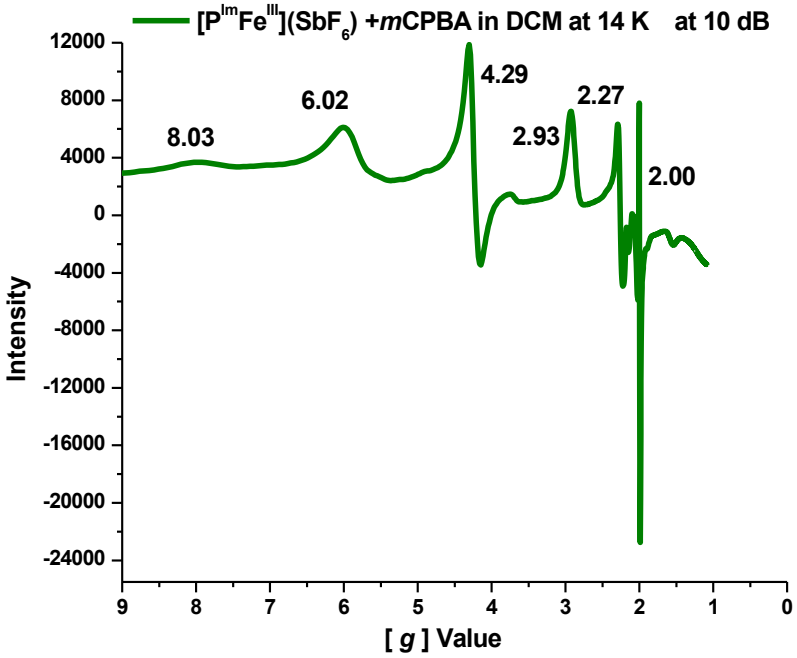

Figure S14. EPR spectrum of the generation of Cmpd-I-type species by addition of *m*CPBA to **(1-SbF$_6$)**.

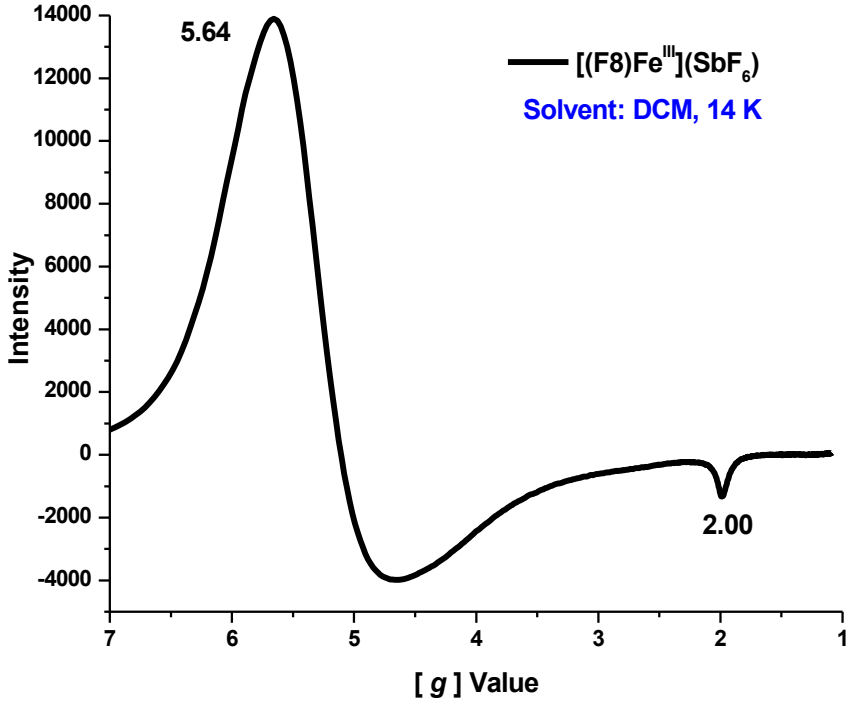

Figure S15. EPR of complex (**5-SbF$_6$**) [3.0 mM] in CH_2Cl_2.

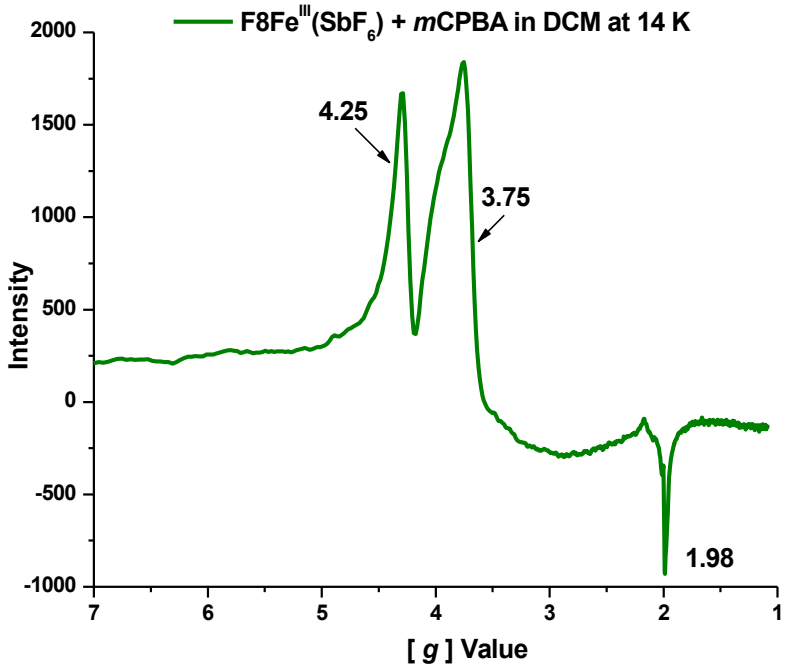

Figure S16. EPR spectrum of the generation of Cmpd-I-type species by addition of *m*CPBA to **(1-SbF$_6$)**.

The second set of samples was prepared under aerobic conditions in a acetonitrile:water (1:1) mixture. 0.57 mL of a complex (**1-OH**) (3.0 mM) solution were placed in two EPR tubes. One of the tubes was frozen in liquid N_2 and the EPR spectrum was recorded (**Figure S17**). The second tube was cooled down to 0 ºC in an ice bath and 0.03 mL of a CAN solution were added. The EPR tube was frozen and the spectrum was recorded at 14K (**Figure S18**). The same procedure was followed for the (**5-OH**) (**Figures S19-S20**). Complex (**1-OH**) showed two set of signals, a 6.04 [g] value which corresponds to an high-spin iron (III) compound and [g] = 2.30, 2.15, 1.98 values which can be assigned to a low-spin iron(III) compound. After addition of CAN, a shift and increase of the [g] = 6.00 and 4.33 signals was observed, which is assigned to the formation of the high-spin iron(III) complex (**4-X**) (green solution). For complex (**5-OH**), [g] values = 6.00 and 4.33 were found, like in the oxidation of (1-OH), signals attributed to the verdoheme-type compound (**4-X**). This extreme was confirmed by recording the EPR spectrum of the isolated compound (**4-X**) in CH_3CN (**Figure S21**), were the same [g] values were observed (6.00, 4.33 and 2.00), which are assigned to a mixture of high-spin iron(III) complexes with different coordination environments (g = 4.33 rhombic complex).

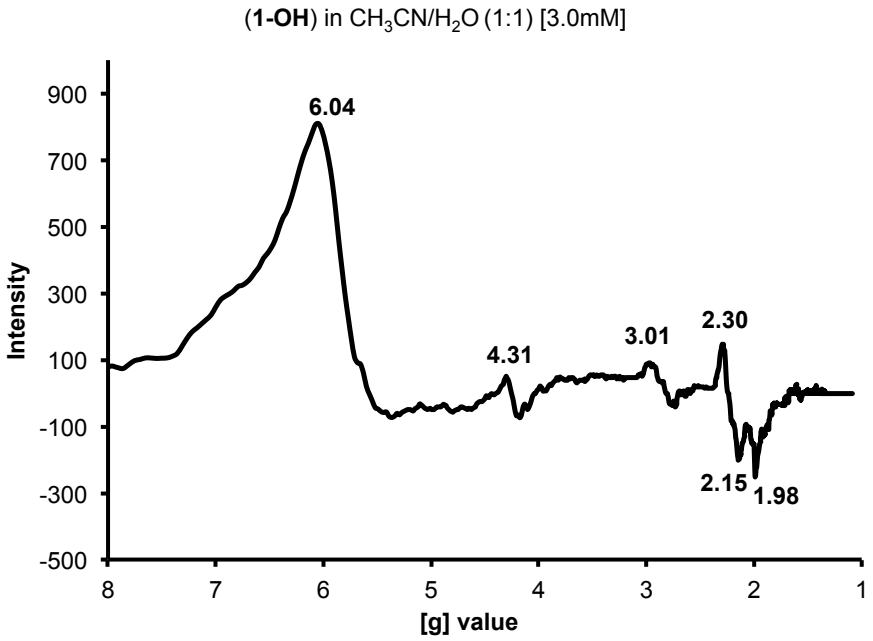

Figure S17. EPR spectrum of **(1-OH)**.

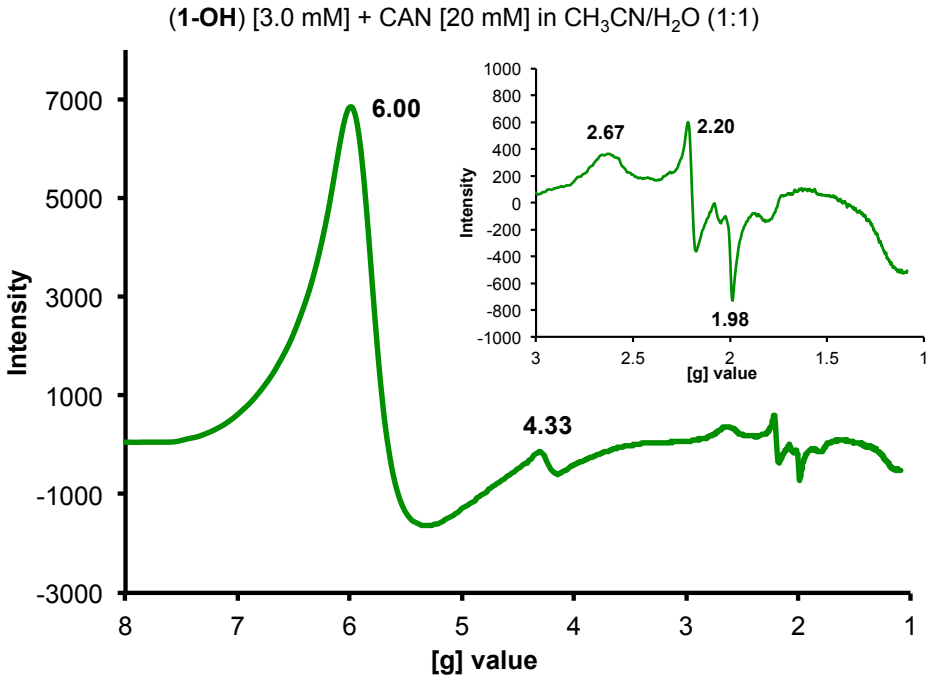

Figure S18. EPR spectrum after addition of CAN [20 mM] to **(1-OH).**

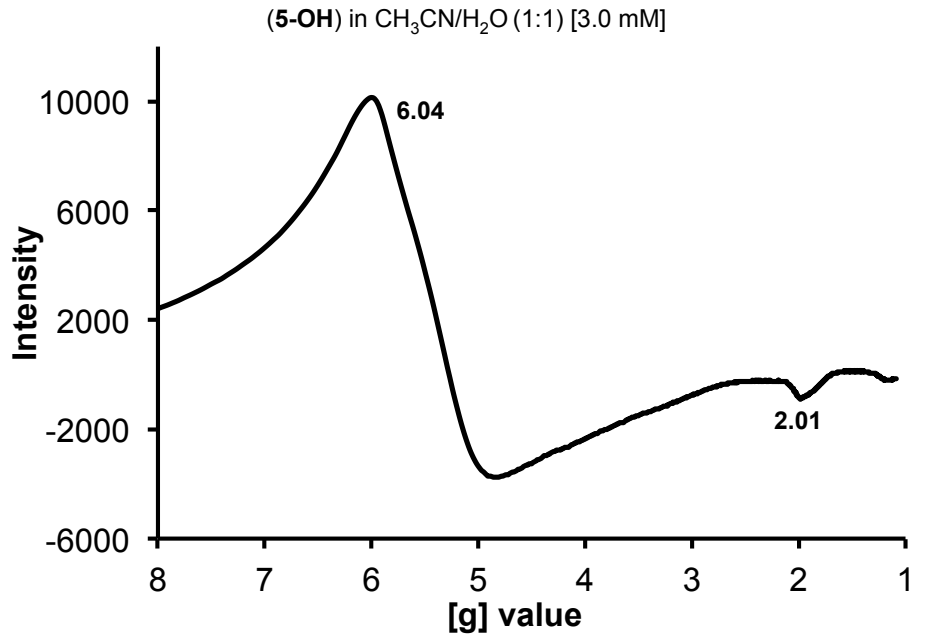

Figure S19. EPR spectrum of **(5-OH)**.

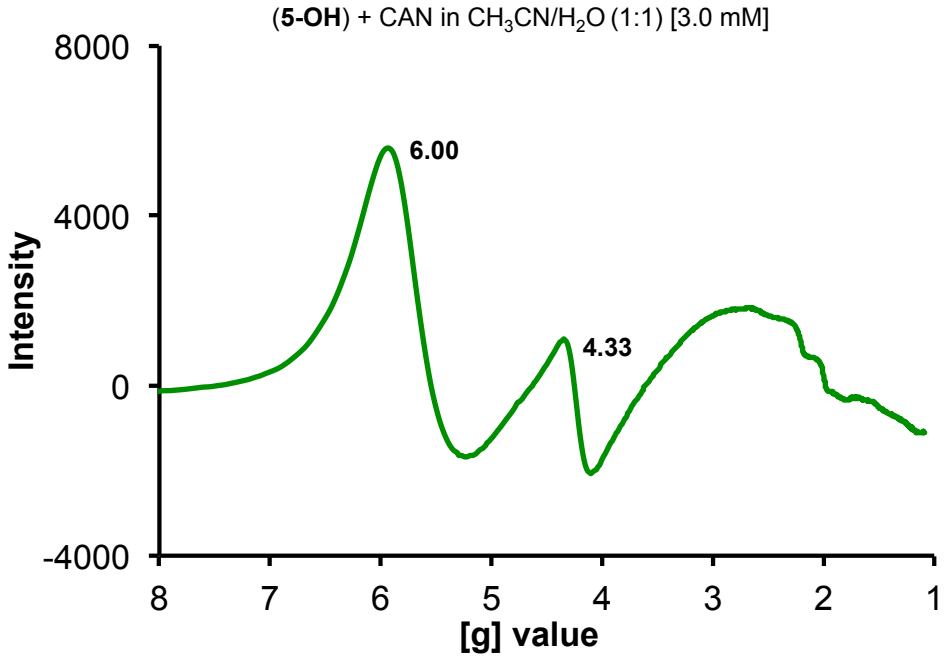

Figure S20. EPR spectrum after addition of CAN [20 mM] to **(5-OH).**

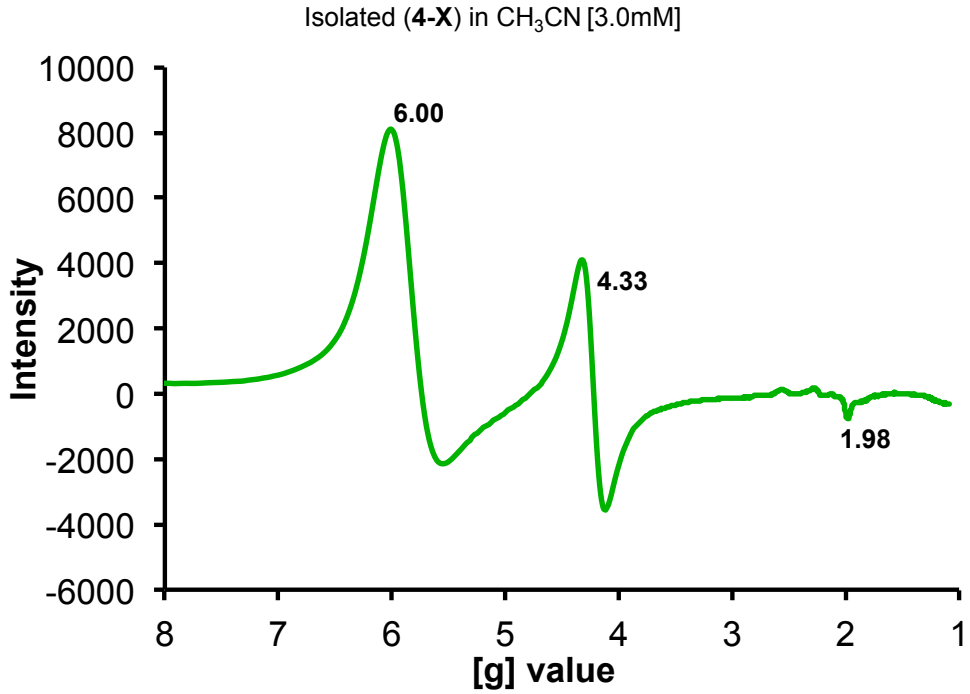

Figure S21. EPR spectrum of the isolated compound (**4-X**) [3 mM] in CH_3CN.

7. ^{2}H-NMR experiments:

0.57 mL of a complex (**$d_8$1-OH**) (3.0 mM) solution (CH_3CN/H_2O; 1:1) were placed in a NMR tube. After cooling down to 0ºC, the desired quantity of CAN was dissolved in 0.1 mL of H_2O and 0.03 mL of this aqueous solution were injected to the tube. Different spectra were recorded for (**$d_8$1-OH**) (**Figure S22**), (**$d_8$1-OH**) after addition of CAN (**Figure S23)** and for the decomposition products (**Figure S24**). For complex (**$d_8$5-OH**), the same procedure was used. As reported before, for complex (**$d_8$5-OH**) a pyrrole signal at 81 ppm was found, which is assigned to a high-spin iron(III) complex.[8] After addition of CAN, a new signal at 62 ppm was formed, assigned to the verdoheme high-spin iron(III) (**4-X**) complex, the same compound formed in the oxidation of (**$d_8$1-OH**) (**Figure S25**). Decomposition of the green complex formed (**4-X**) to a brown solution showed a pyrrole signal at 4.4 ppm, which can be assigned as a pyrrolic organic compound after release of iron of verdoheme (**4-X**).

(**1-OH**) in CH_3CN/H_2O [3.0 mM]

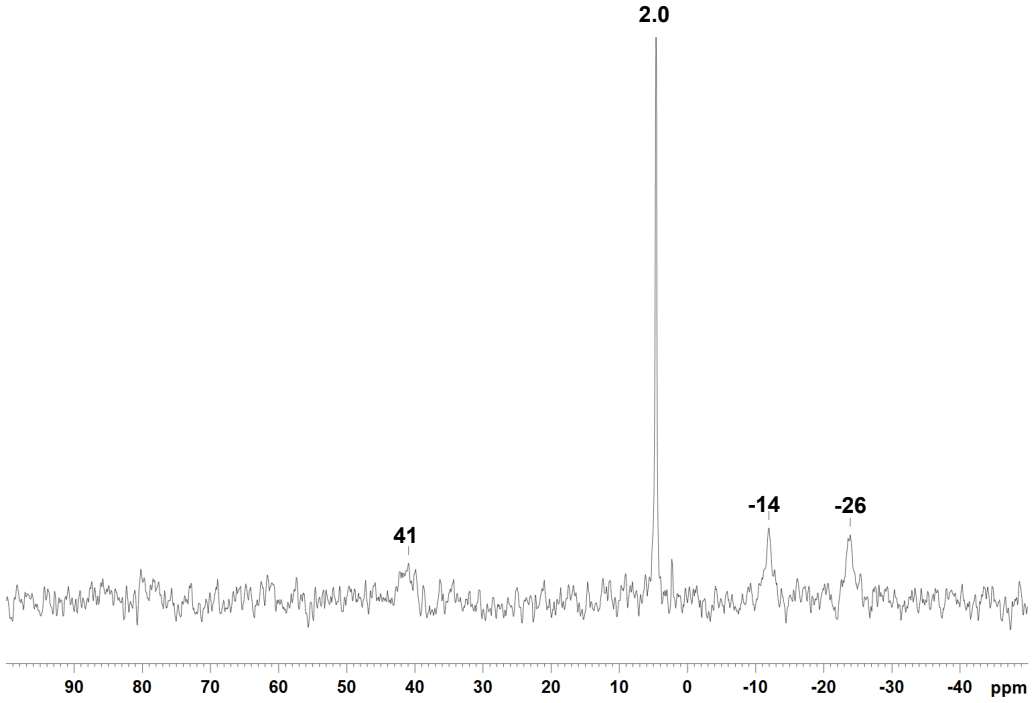

Figure S22. ^{2}H-NMR of complex **(1-OH)** [3.0 mM] in a CH_3CN/H_2O mixture (1:1).

(**1-OH**) in CH_3CN/H_2O [3.0 mM] + CAN [20 mM]

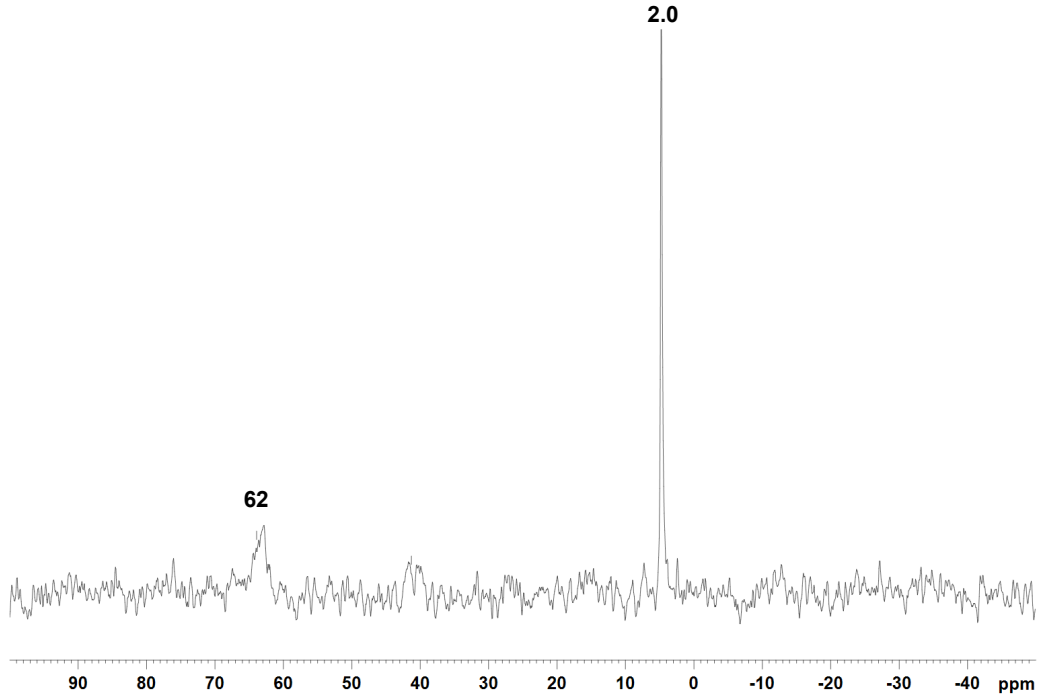

Figure S23. ^{2}H-NMR of complex **(1-OH)** [3.0 mM] in a CH_3CN/H_2O mixture (1:1) after addition of CAN [20 mM] (green complex (**4-X**)).

(**1-OH**) in CH_3CN/H_2O [3.0 mM] + CAN [20 mM] (decay)

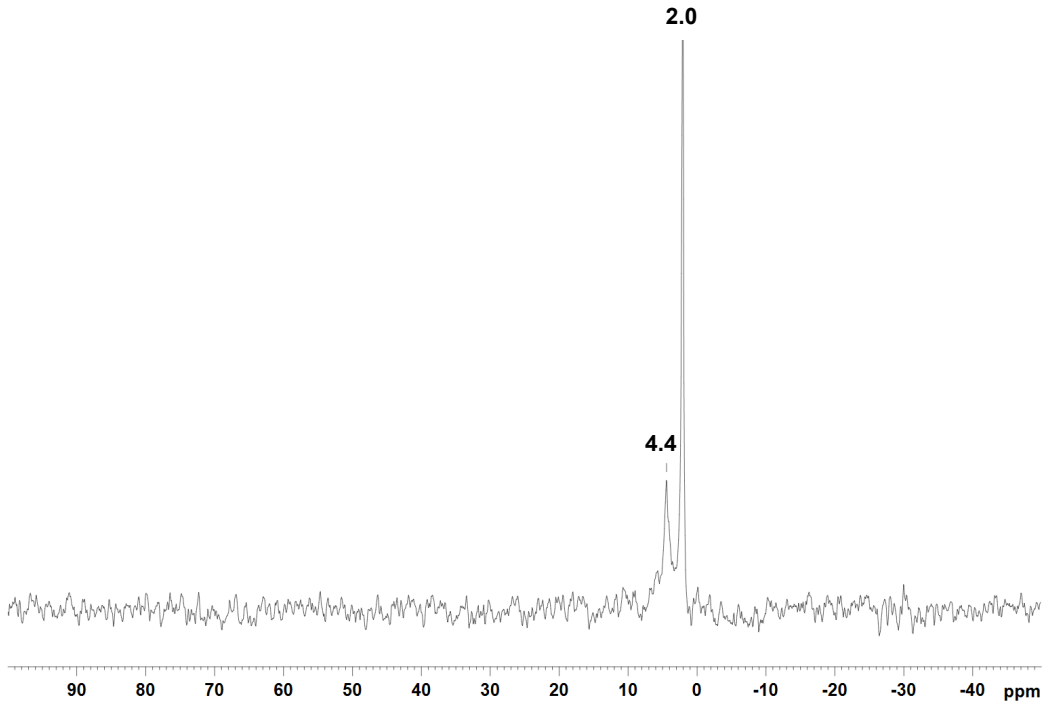

Figure S24. ^{2}H-NMR of complex **(1-OH)** [3.0 mM] in a CH_3CN/H_2O mixture (1:1) after addition of CAN [20mM] and its decay (brown compound).

(**5-OH**) in CH_3CN/H_2O [3.0 mM] + CAN [20 mM]

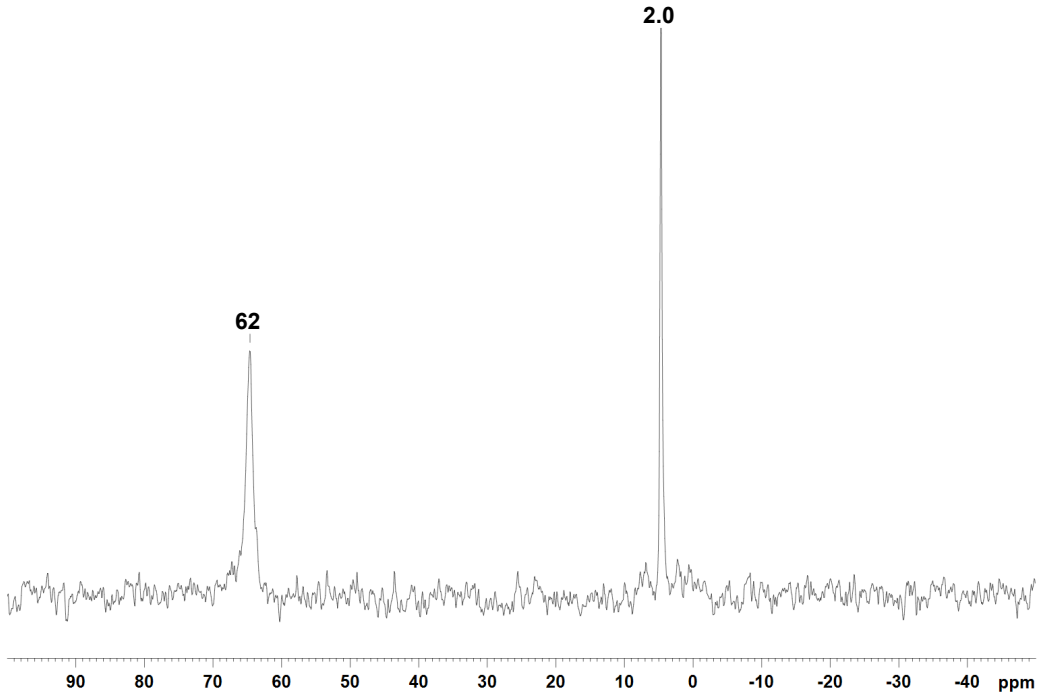

Figure S25. ^{2}H-NMR of complex **(1-OH)** [3.0 mM] in a CH_3CN/H_2O mixture (1:1) after addition of CAN [20 mM] (green complex (**4-X**)).

8. ESI-MS experiments:

Two different sets of conditions were used to follow the reactions by ESI-MS. One is the direct injection of the crude reaction mixture, where the initial concentration of (**1-OH**) and (**5-OH**) were [0.1 mM]. The second procedure employed was injection of different aliquots of the crude reaction mixture after being quenched under different conditions. No differences in reaction intermediates and final products were observed between the different injection conditions. All the masses observed were corrected based on the signal of the internal CsI standard. The reaction mixture was prepared as for in typical UV-Vis experiments. After cooling to 0 ºC 1 mL of a complex (**1-OH**) [0.1 mM] solution (CH_3CN/H_2O; 1:1), CAN [10 mM] was added and direct injection of the reaction mixuture was carried out. **Figure S26** shows the formation of (**1+2O**) (m/z = 1007.1) from (**1**) (m/z = 975.5, protonated complex) (top spectrum) during the first minute of reaction. After 5 minutes (bottom spectrum), (**1**) and (**1+2O**) transformed, leading to formation of verdoheme complex (**4-X**) (m/z = 703.4, 719.6, 738.3, 764.9) and (**TA+O**) (m/z = 304.0).

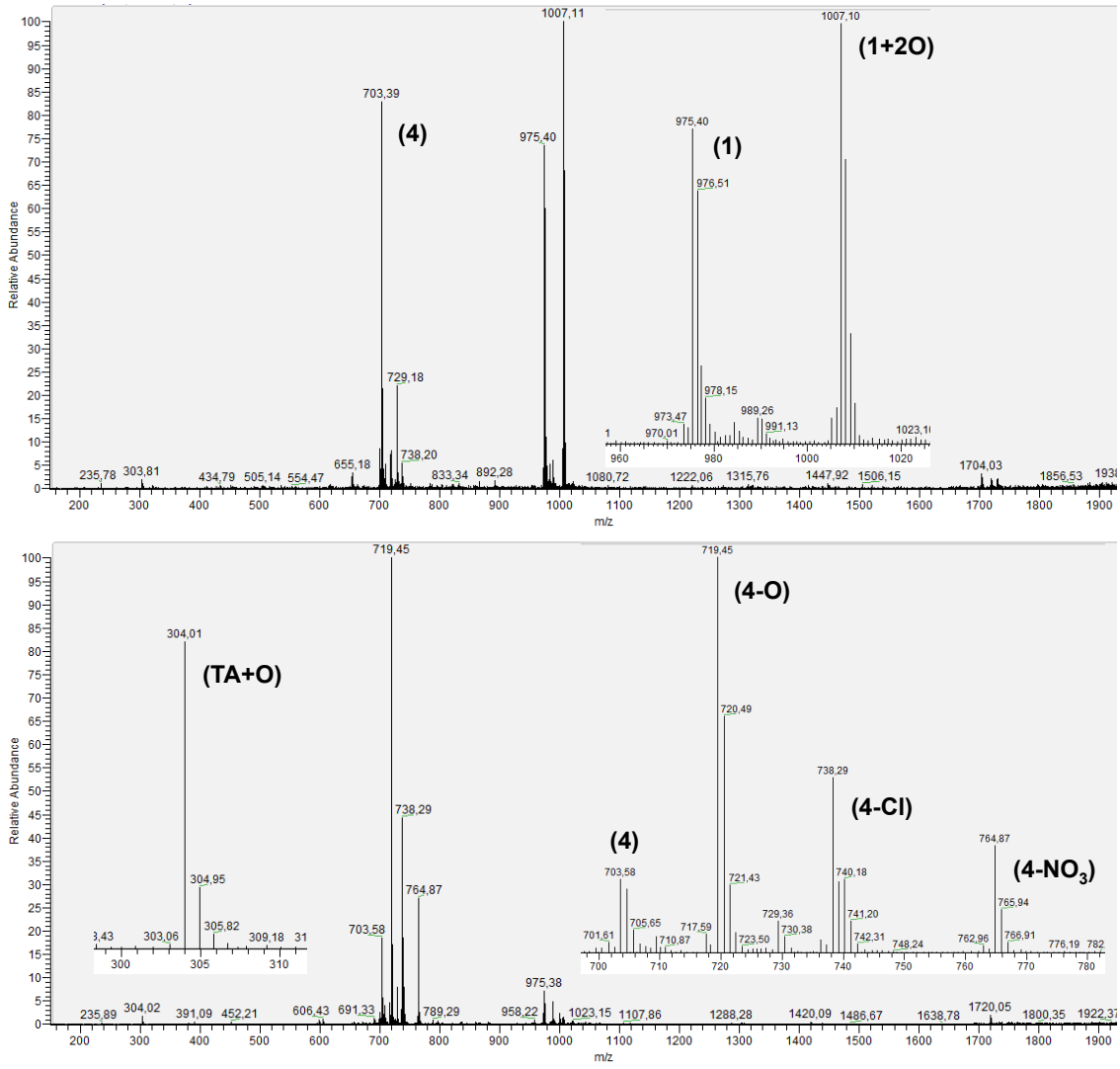

Figure S26. ESI-MS spectra for the oxidation of (**1-OH**) with CAN [10 mM] in a (CH_3CN/H_2O) (direct injection of the reaction mixture). Top spectrum: average of the first reaction minute. Bottom spectrum: average spectrum from 5-10 minutes after addition of CAN.

After cooling to 0 ºC 1 mL of a complex (**1-OH**) [0.1 mM] solution ($CH_3CN/H_2{}^{18}$**O**; 1:1), CAN [10 mM] was added and direct injection of the reaction mixture was carried out. **Figure S27** shows the formation of (**1+2**^{18}**O**) (m/z = 1011.1) from (**1**) (m/z = 975.6, protonated complex) (top spectrum) during the first minute of reaction. After 5 minutes (bottom spectrum), (**1**) and (**1+2**^{18}**O**) have decomposed leading to the formation of the verdoheme complex (**4**^{18}**O-X**) (m/z = 705.6, 721.5, 740.1, 766.8) and (**TA+**^{18}**O**) (m/z = 306.0). More than 90% of 18-oxygen incorporation was observed in the formation of (**1+2**^{18}**O**), (**4**^{18}**O-X**) and (**TA+**^{18}**O**).

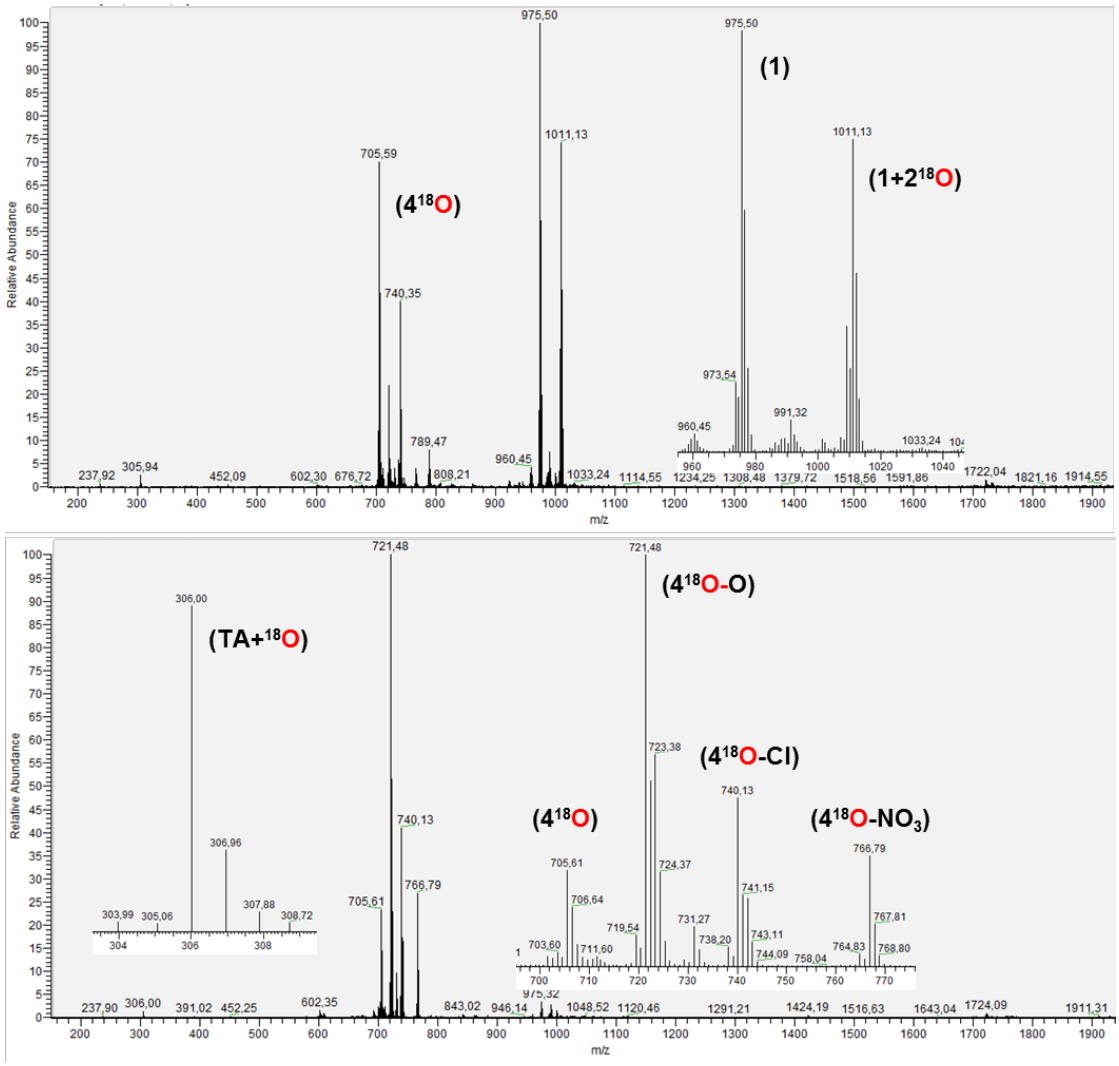

Figure S27. ESI-MS spectra for the oxidation of (**1-OH**) with CAN [10 mM] in a ($CH_3CN/H_2{}^{18}$**O**) (direct injection of the reaction mixture). Top spectrum: average of the first reaction minute. Bottom spectrum: average spectrum from 5-10 minutes after addition of CAN.

After cooling to 0 ºC 1 mL of a complex (**1-OH**) [0.1 mM] solution ($CH_3CN/H_2O/H_2{}^{18}$**O**; 1:0.5:0.5), CAN [10 mM] was added and direct injection of the reaction mixture was carried out. **Figure S28** shows the formation of (**1+2O**) (m/z = 1007.1), (**1+2^{16}O^{18}O**) (m/z = 1009.1) (**1+2^{18}O**) (m/z = 1011.1) in a 1:2:1 ratio, from (**1**) (m/z = 975.8, protonated form) (top spectrum) during first minute of reaction. After 5 minutes (bottom spectrum), (**1**), (**1+2O**), (**1+2^{16}O^{18}O**) and (**1+2^{18}O**) were transformed leading to the formation of verdoheme-type complexes (**4-X**) (m/z = 703.4, 719.6, 738.3, 764.9), (**4^{18}O-X**) (m/z = 705.6, 721.5, 740.2, 766.9), (**TA+O**) (m/z = 304.0) and (**TA-^{18}O**) (m/z = 306.0) and in a 1:1 ratio, showing 50% of 18-oxygen incorporation into reaction products.

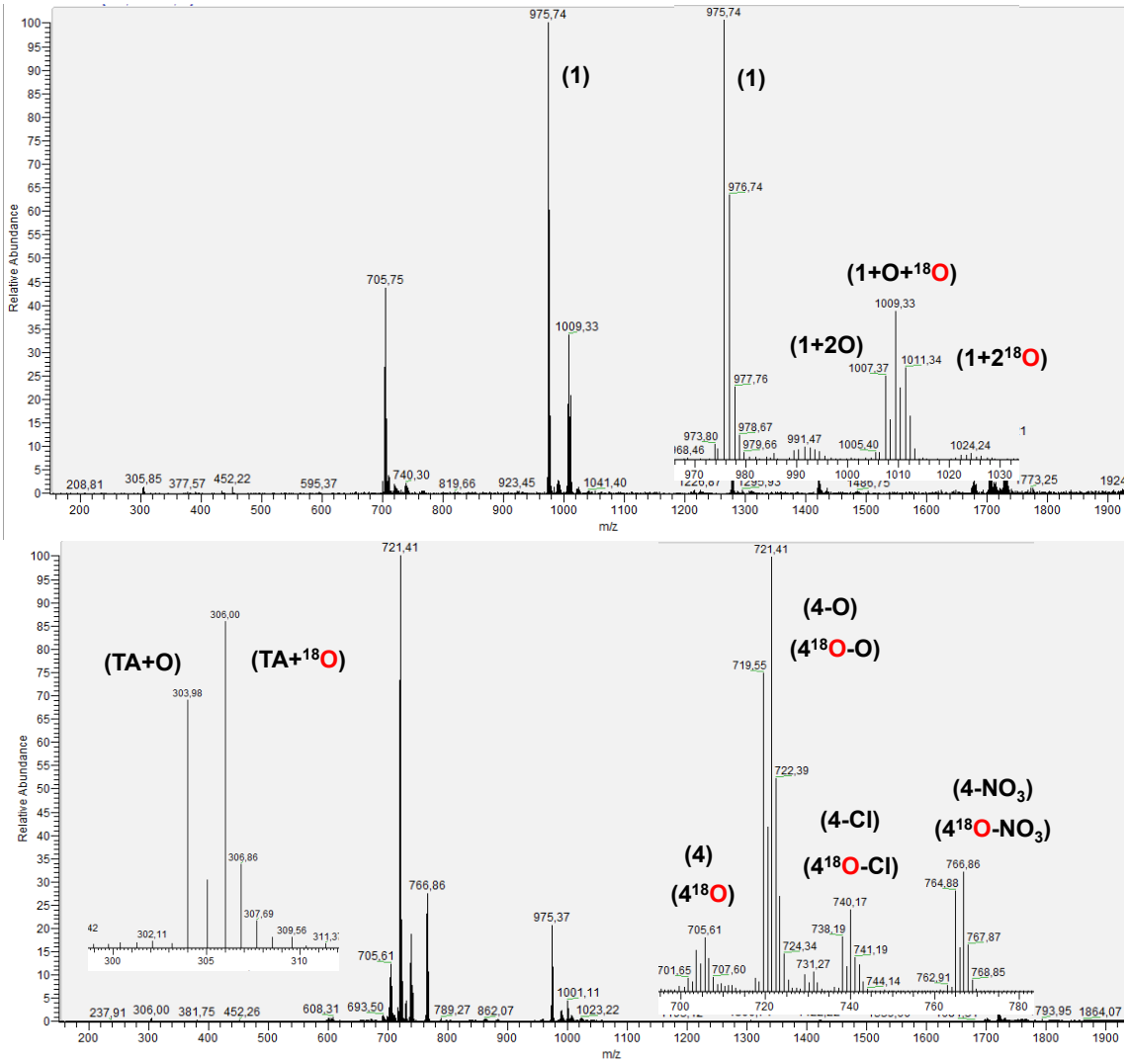

Figure S28. ESI-MS spectra for the oxidation of (**1-OH**) with CAN [10 mM] in a ($CH_3CN/H_2O/H_2{}^{18}O$) (1:0.5:0.5) (direct injection of the reaction crude). Top spectrum: average of the first reaction minute. Bottom spectrum: average spectrum from 5-10 minutes after addition of CAN.

Into a round bottom flask saturated with an $^{18}O_2$ atmosphere and containing CAN, 1 mL of a complex (**1-OH**) [0.1 mM] solution (CH_3CN/H_2O, previously degassed by several Ar/vacumm cycles) was added. Then, direct injection of the reaction mixture was carried out. **Figure S29** shows the formation of (**1+2O**) (m/z = 1007.1), from (**1**) (m/z = 975.6, protonated complex) (top spectrum) during first minute of reaction. After 5 minutes (bottom spectrum), (**1**) and (**1+2O**) were transformed leading to the formation of verdoheme complexes (**4-X**) (m/z = 703.4, 719.6, 738.3, 764.9) and (**TA+O**) (m/z = 304.0) showing no 18-oxygen incorporation into reaction products.

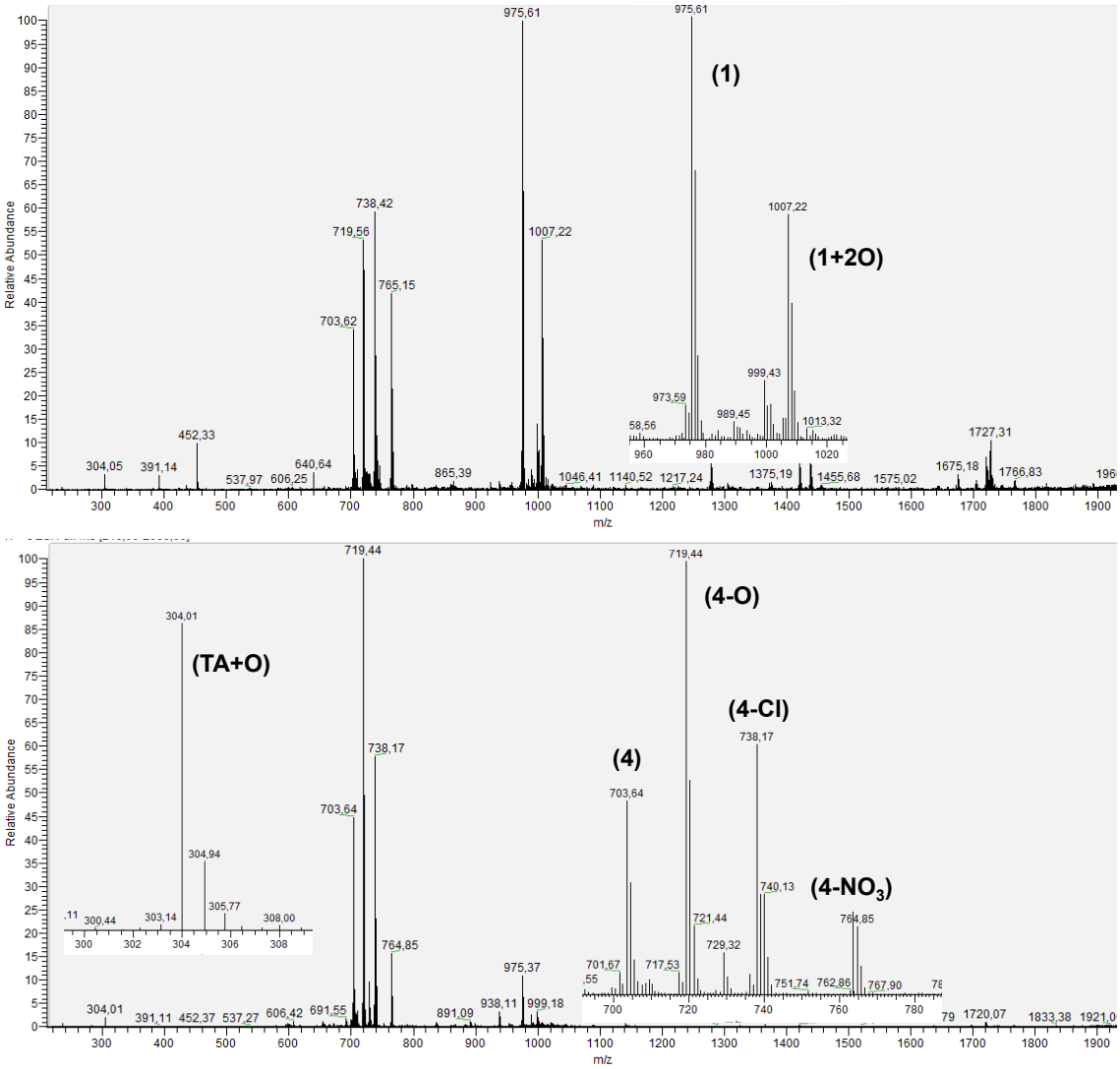

Figure S29. ESI-MS spectra for the oxidation of (**1-OH**) with CAN [10 mM] in a (CH_3CN/H_2O) in a saturated $^{18}\mathbf{O}_2$ atmosphere (direct injection of the reaction mixture). Top spectrum: average of the first reaction minute. Bottom spectrum: average spectrum from 5-10 minutes after addition of CAN.

After cooling down to 0ºC 1mL of a complex (**1-OH**) [0.1 mM] solution (CH_3OH/H_2O; 1:1), CAN [40 mM] was added and direct injection of the reaction crude was carried out. **Figure S30** shows the formation of (**1+2O**) (m/z = 1007.1) from (**1**) (m/z = 975.5, protonated complex) (top spectrum) but also the formation of (**1+(O)(OMe)**) (m/z = 1022.1) which would correspond to the benzoyl-biliverdin-type compound formed by addition of one molecule of methanol and molecule of water into (**1**) during first minute of reaction. 5 minutes (bottom spectrum), (**1**) and (**1+2O**) and (**1+O(OMe)**) were transformed, leading to the formation of verdoheme complex (**4-X**) (m/z = 703.4, 719.6, 738.3, 764.9), (**TA+O**) (m/z = 304.0) but also (**TA+(O)(OMe)**), resulting from the addition of MeOH and water to the tethered arm (m/z = 336.2, protonated form).

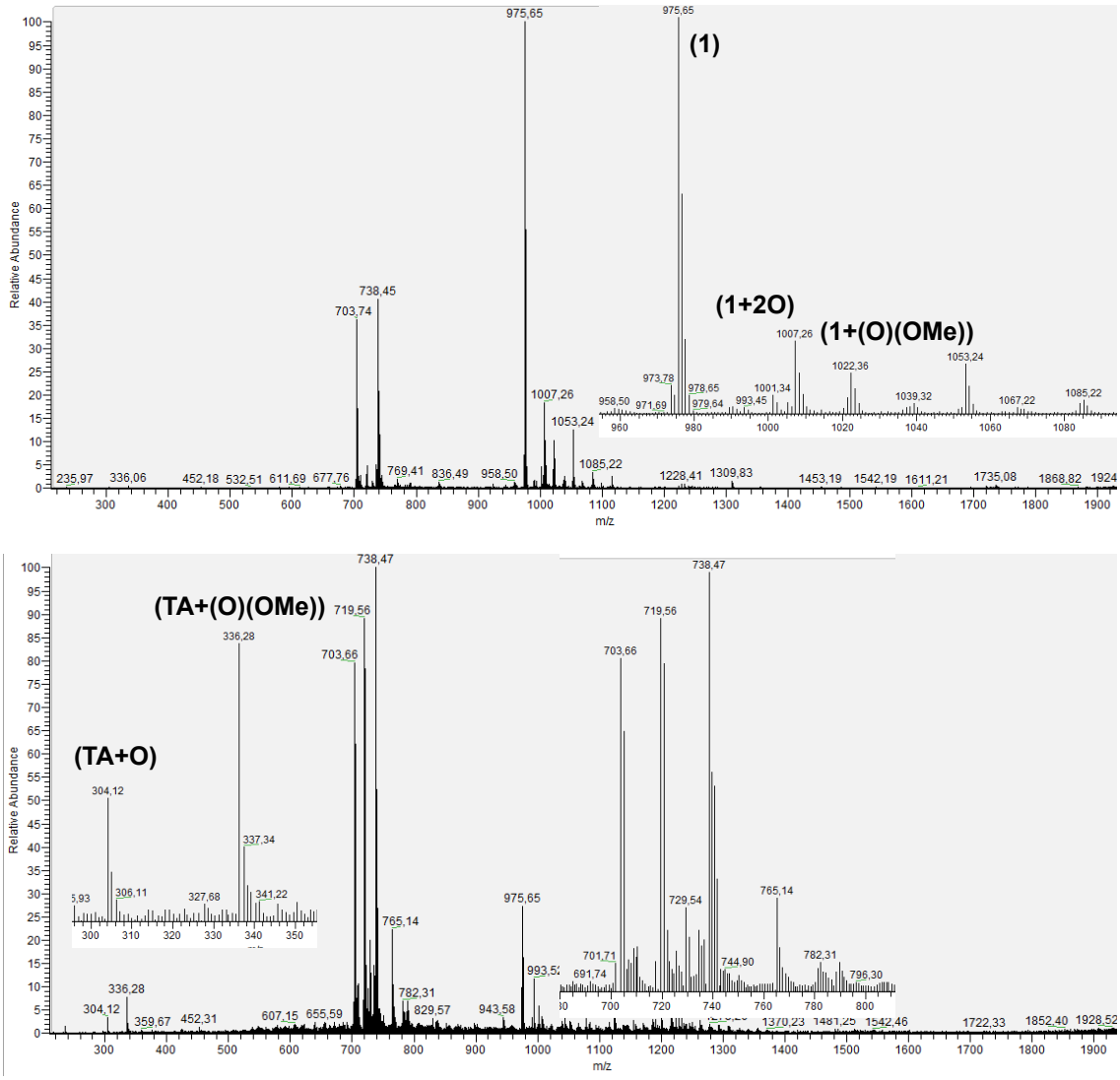

Figure S30. ESI-MS spectra for the oxidation of (**1-OH**) with CAN [40 mM] in a (CH_3OH/H_2O) (direct injection of the reaction crude). Top spectrum: average of the first reaction minute. Bottom spectrum: average spectrum from 1 to 5 minutes after addition of CAN.

After cooling down to 0ºC 1mL of a complex (**1-OH**) [0.1 mM] solution (CH_3OH), CAN [40 mM] was added and direct injection of the reaction crude was carried out. **Figure S31** shows no formation of (**1+2O**) (m/z = 1007.1) from (**1**) (m/z = 975.5, protonated complex) (top spectrum) during first minute of reaction and no other peaks corresponding to the isoporphyrin nor benzoyl-biliverdin intermediates. After 5 minutes (bottom spectrum), (**1**) was fully transformed, leading to the formation of biliverdin complex resulting from the attack of MeOH (m/z = 734.3) and (**TA+(OMe)$_2$**), resulting from the addition of MeOH to the tethered arm (m/z = 350.2). Other peaks are observed, pointing out that the reaction is not as clean as in the case of water.

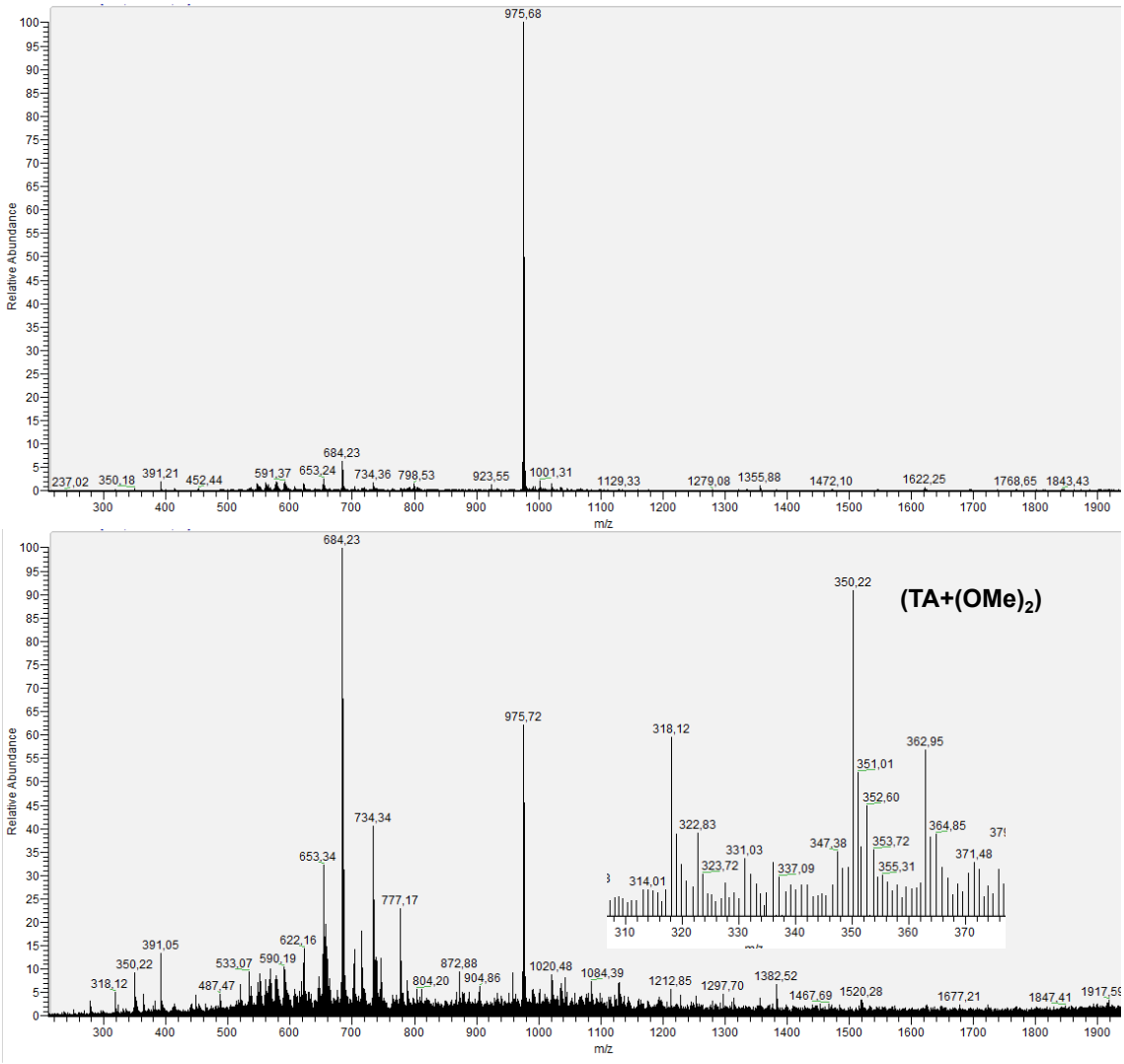

Figure S31. ESI-MS spectra for the oxidation of (**1-OH**) with CAN [40 mM] in a (CH_3CN /CH_3OH) (direct injection of the reaction crude). Top spectrum: average of the first reaction minute. Bottom spectrum: average spectrum from 1 to 5 minutes after addition of CAN.

After cooling to 0 ºC 1mL of a complex (**5-OH**) [0.1 mM] solution (CH_3CN/H_2O; 1:1), CAN [40 mM] was added and direct injection of the reaction mixture was carried out. **Figure S32** shows the formation of (**5-O**) (m/z = 828.5), (**5-Cl**) (m/z = 847.3) and (5-NO_3) (m/z = 874.0) from (**5**) (m/z = 812.8, protonated complex) (top spectrum) during first minute of reaction. After 5 minutes (bottom spectrum), (**5**) led to the leading to the formation of verdoheme complex (**4-X**) (m/z = 703.4, 719.6, 738.3, 764.9) like in complex (**1**). As expected, no formation of (**TA+O**) (m/z = 304.0) was observed. Labeling studies (**Figure S33**) using $H_2{}^{18}O$ confirm that (**5-O**) is observed due to the cleavage of the (**5-NO_3**) species, because no incorporation of water is observed. On the other hand, we observed incorporation of 18-oxygen into the verdoheme species (**4-X**) although in a lower percentage (<75%), maybe due to the strongest conditions (higher CAN concentration) used in the (**5-OH**) oxidation chemistry.

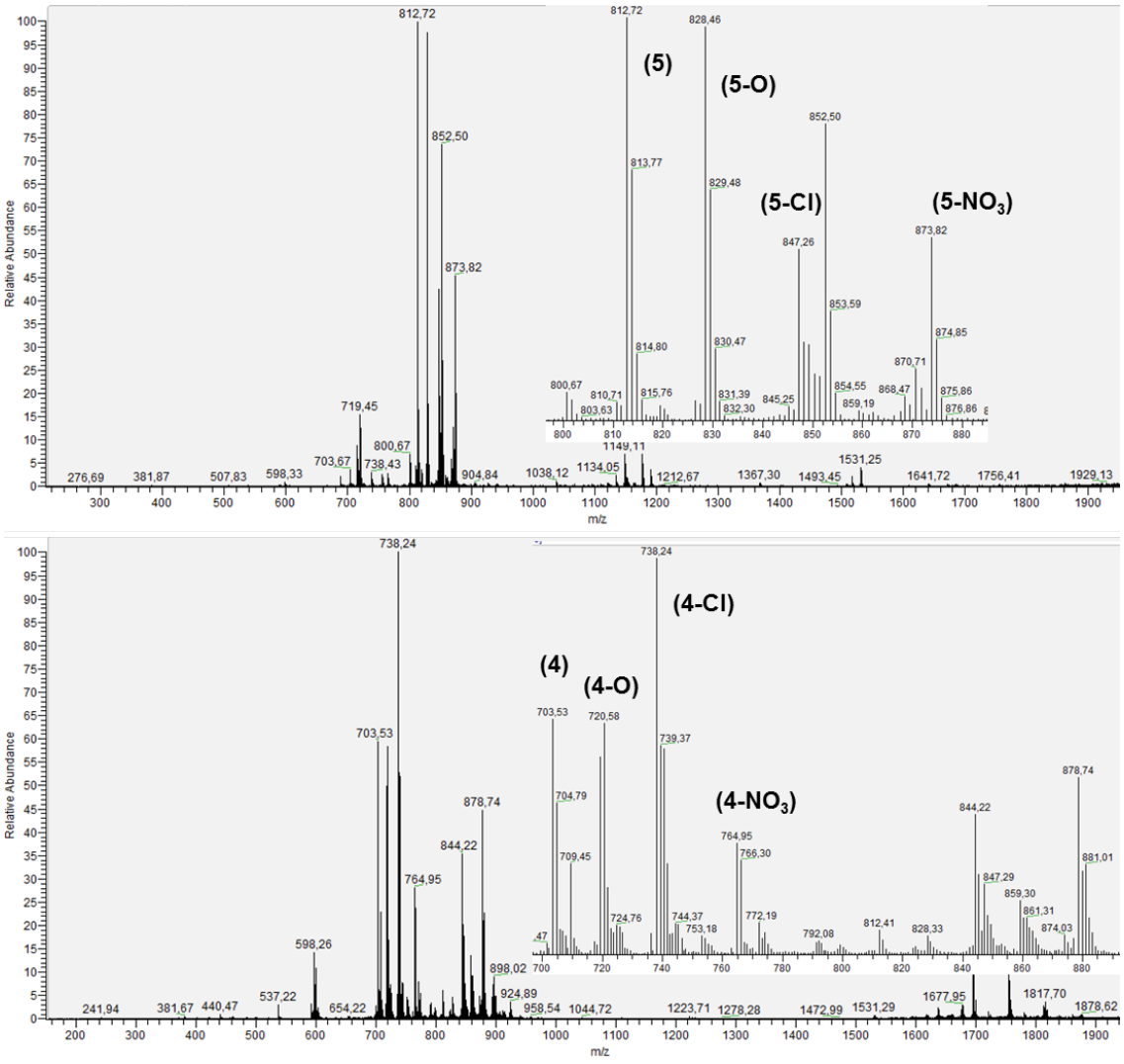

Figure S32. ESI-MS spectra for the oxidation of (**5-OH**) with CAN [40 mM] in a (CH_3CN/H_2O) (direct injection of the reaction mixture). Top spectrum: average of the first reaction minute. Bottom spectrum: average spectrum from 5-10 minutes after addition of CAN.

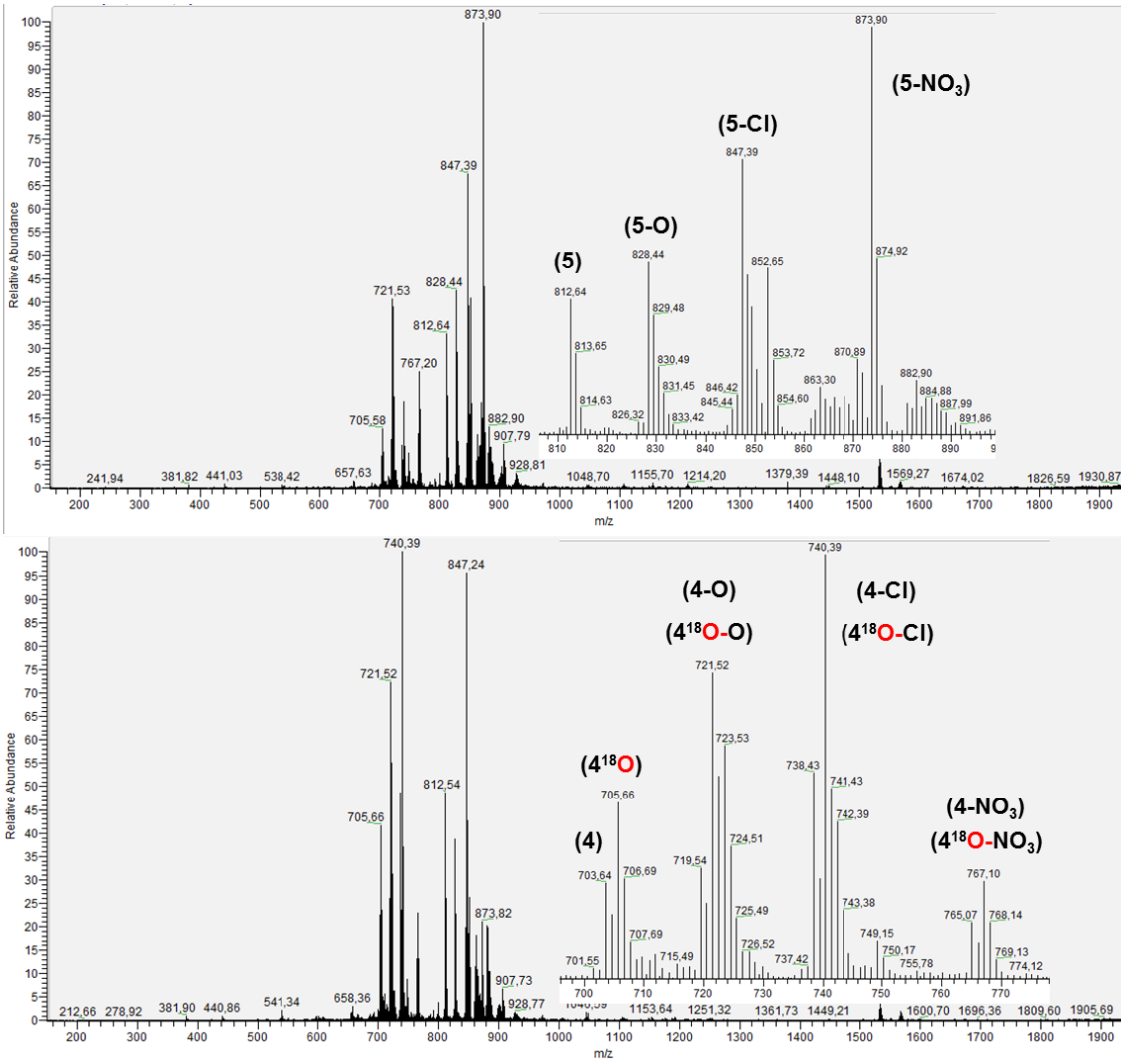

Figure S33. ESI-MS spectra for the oxidation of (**5-OH**) with CAN [40 mM] in a ($CH_3CN/H_2{}^{18}O$) (direct injection of the reaction mixture). Top spectrum: average of the first reaction minute. Bottom spectrum: average spectrum from 5-10 minutes after addition of CAN.

9. References

(1) Ghiladi, R. A.; Kretzer, R. M.; Guzei, I.; Rheingold, A. L.; Neuhold, Y.-M.; Hatwell, K. R.; Zuberbühler, A. D.; Karlin, K. D. *Inorg. Chem.* **2001**, *40*, 5754.
(2) Li, Y.; Sharma, S. K.; Karlin, K. D. *Polyhedron* **2012**.
(3) Nam, W.; Park, S.-E.; Lim, I. K.; Iim, m. H.; Hong, J.; Kim, K. *J. Am. Chem. Soc.* **2003**, *125*, 14674.
(4) Green, M. T.; Dawson, J. H.; Gray, H. B. *Science* **2004**, *304*, 1653.
(5) Rittle, J.; Green, M. T. *Science* **2010**, *330*, 933.
(6) Takahashi, A.; Kurahashi, T.; Fujii, H. *Inorg. Chem.* **2011**, *50*, 6922.
(7) Takahashi, A.; Kurahashi, T.; Fujii, H. *Inorg Chem* **2009**, *48*, 2614.
(8) Kopf, M.; Neuhold, Y.; Zuberbuhler, A. D.; Karlin, K. D. *Inorg. Chem.* **1999**, *38*, 3093.